Analytical SEM:
EDX, WDX, EBSD

karsten.kunze (at) scopem.ethz.ch

ETH zürich ScopeM

Analytical SEM

1. Introduction

2. X-ray spectroscopy
   a) Emission of X-rays
   b) Detection of X-rays (EDX)
   c) Detection of X-rays (WDX)

3. Electron back scatter diffraction (EBSD)
   a) general basics
   b) recent developments

Interaction of electrons with matter

- **Elastic** interactions = energy preserved
  - with nuclei (Rutherford scattering):
    - high angle scattering
    - backscattered electrons
    - interference = diffraction
- **Inelastic** interactions = energy reduced
  - with inner shell electrons: - ionisation (X-rays, Auger)
  - with Coulomb potential: - Bremsstrahlung
  - with phonons (crystal lattice oscillations):
    - heat
  - with free electrons in conduction (and valence) bands:
    - secondary electrons
    - plasmons
    - visible light

High energy (primary beam) ~ keV >>

Low energy ~ eV

Interaction of electrons with matter

- **Elastic** interactions = energy preserved
  - with nuclei (Rutherford scattering):

	- high angle scattering	*STEM-HAADF*
	- backscattered electrons	*BSE imaging*
	- interference = diffraction	*EBSD, ECCI*

- **Inelastic** interactions = energy reduced

– with inner shell electrons:	- ionisation (X-rays, Auger)	*X-ray spectroscopy*
– with Coulomb potential:	- Bremsstrahlung	
– with phonons (crystal lattice oscillations):		
	- heat	
– with free electrons in conduction (and valence) bands:		
	- secondary electrons	*SE imaging*
	- plasmons	*EELS*
	- visible light	*cathodo-luminescence*

Multi-modal imaging & analysis

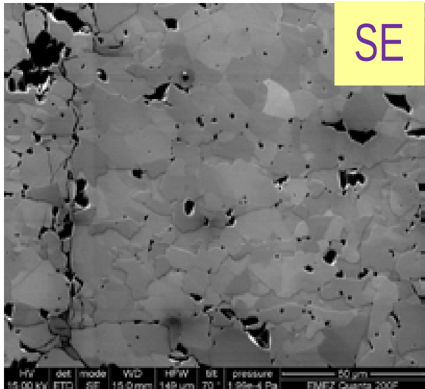

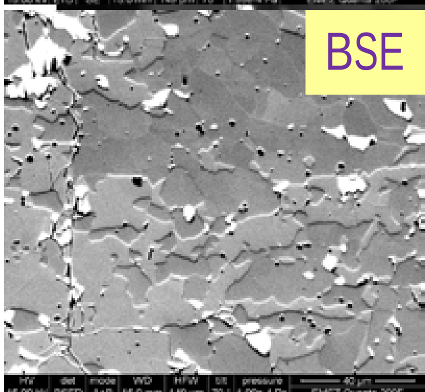

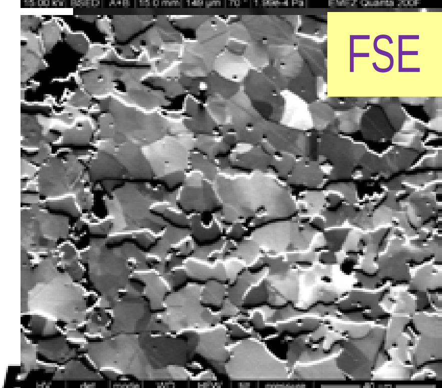

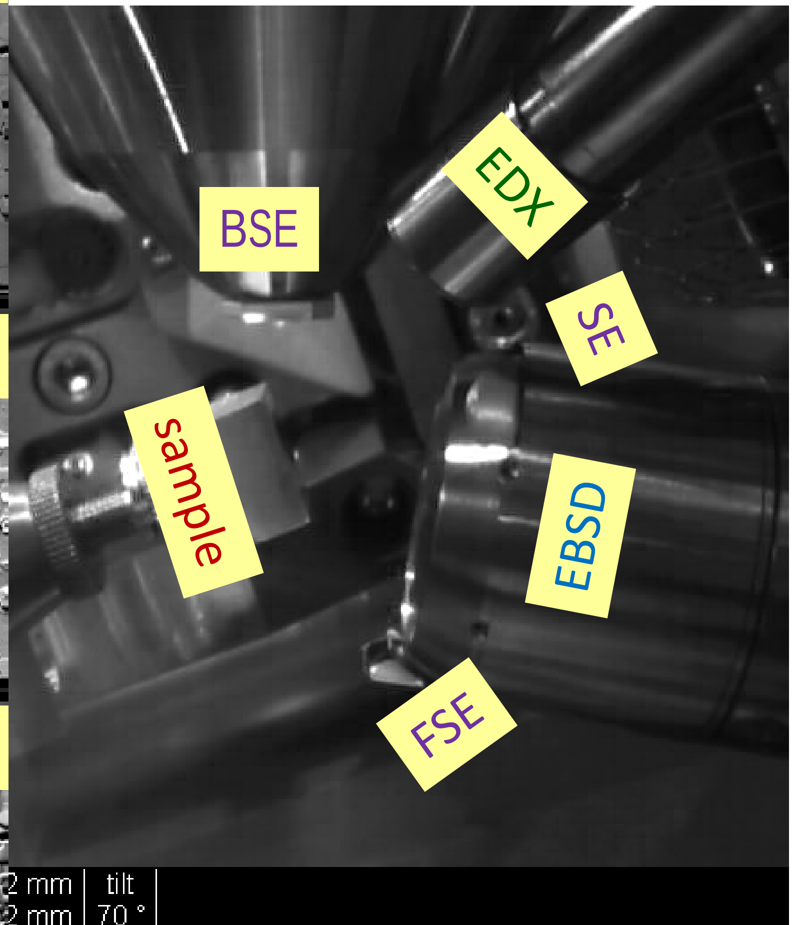

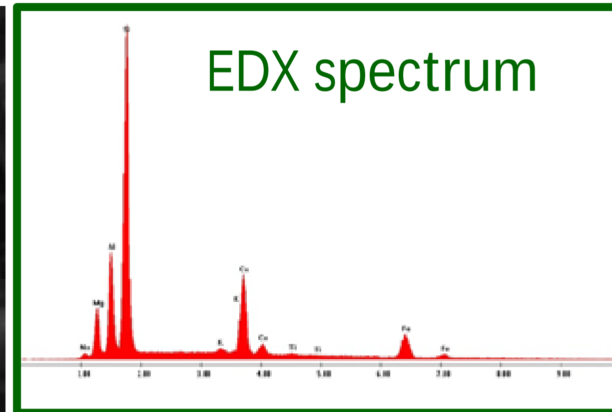

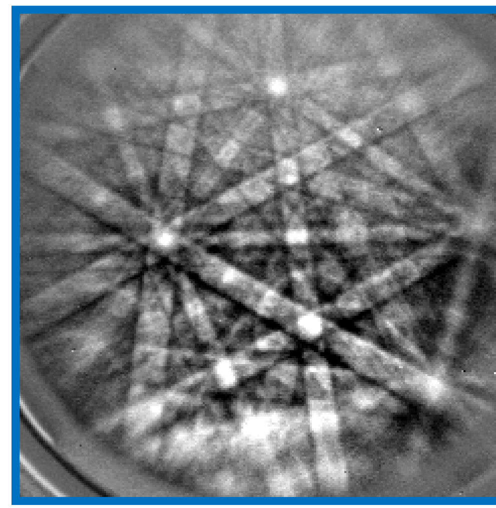

Electron backscatter diffraction pattern

Enstatite reaction rim between quartz and forsterite

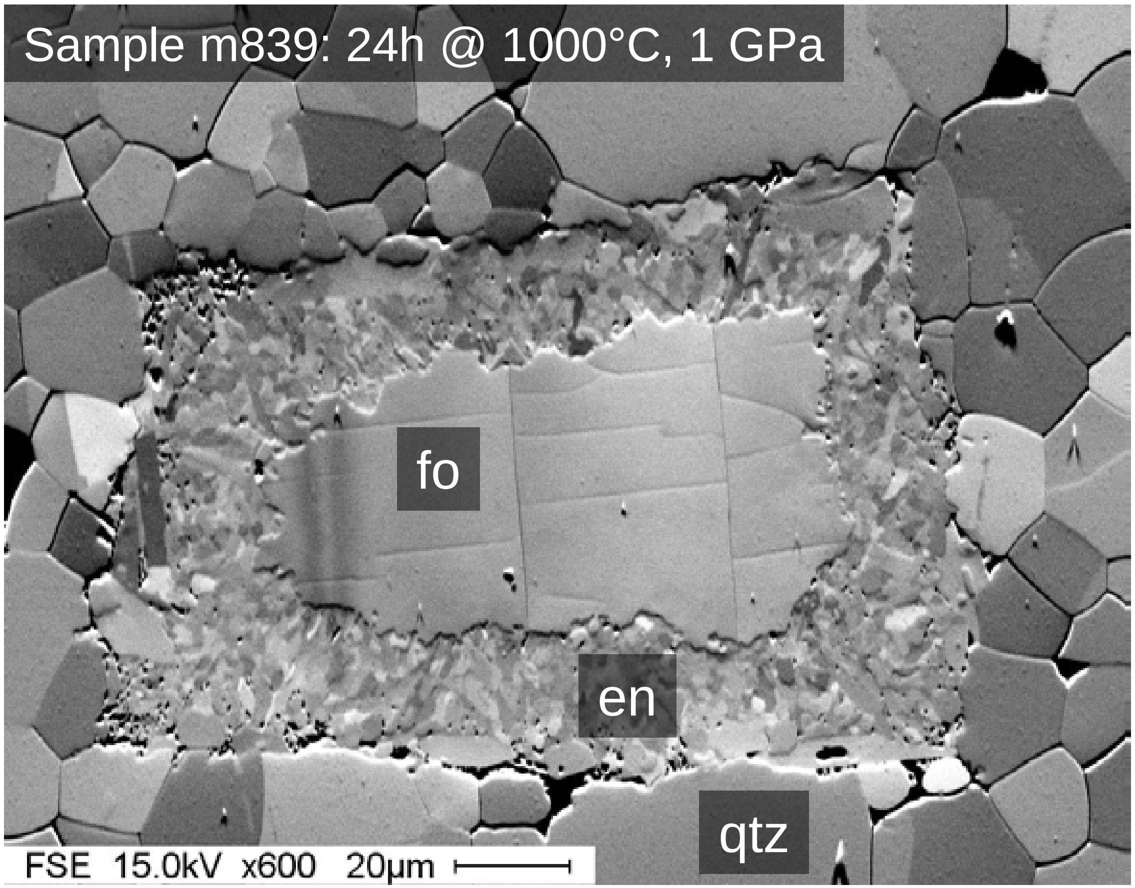

$Mg_2SiO_4 + SiO_2 = 2\ MgSiO_3$

BSE image:
Z contrast

FSE image:
orientation contrast

Abart, Kunze, Milke et al. (2004)
Contrib Mineral Petrol *147,* *633-646*

quartz - enstatite - forsterite

SiO_2	$MgSiO_3$	Mg_2SiO_4
$Z_{avg} = 10.8$	$Z_{avg} = 10.7$	$Z_{avg} = 10.6$

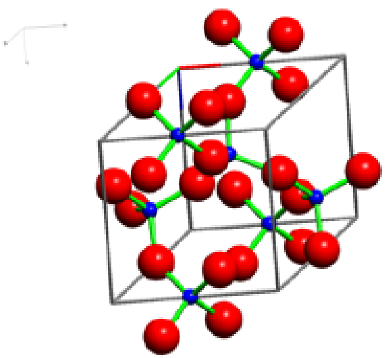
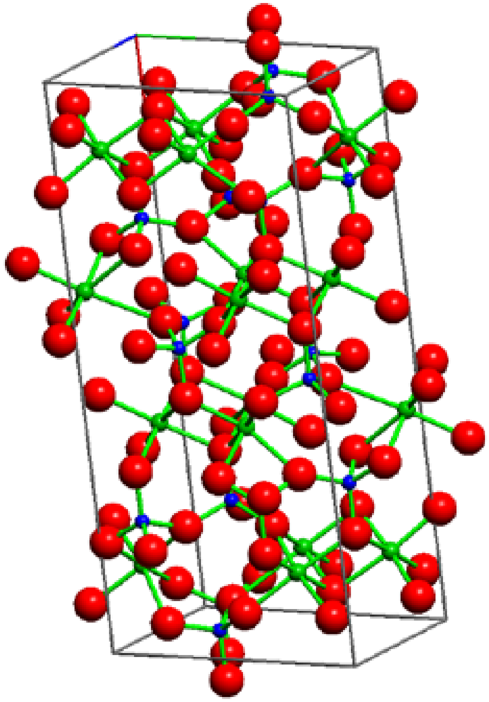
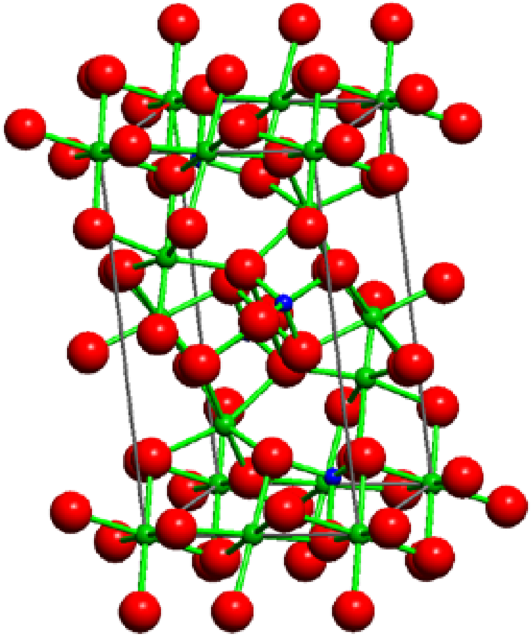

trigonal	orthorhombic	orthorhombic
S.G. 154 = $P3_221$	S.G. 61 = Pbca	S.G. 62 = Pbnm

quartz - enstatite - forsterite

SiO_2

Z_{avg} = 10.8

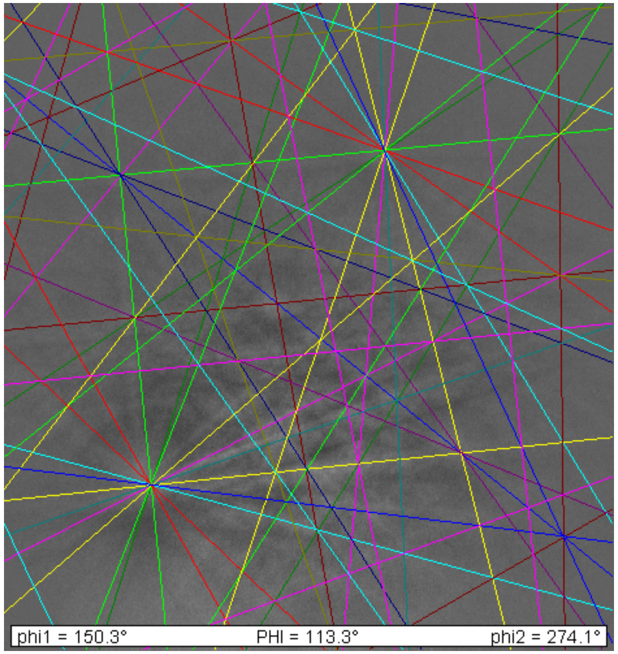

trigonal

S.G. 154 = $P3_221$

$MgSiO_3$

Z_{avg} = 10.7

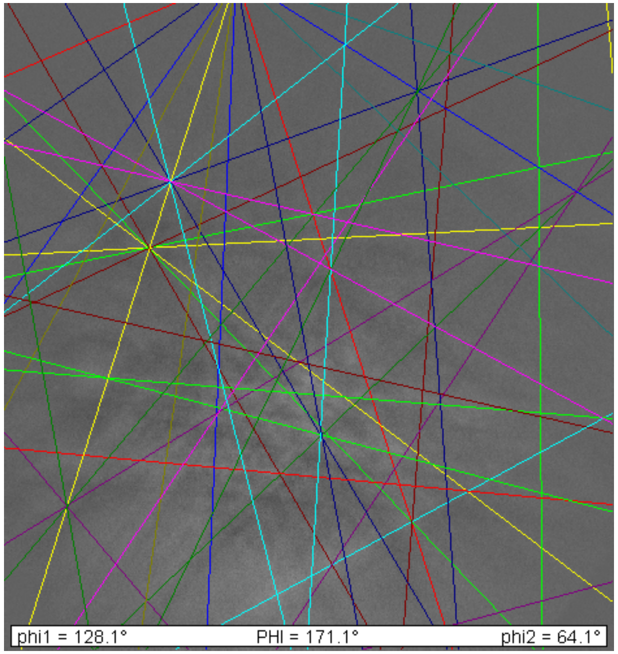

orthorhombic

S.G. 61 = Pbca

Mg_2SiO_4

Z_{avg} = 10.6

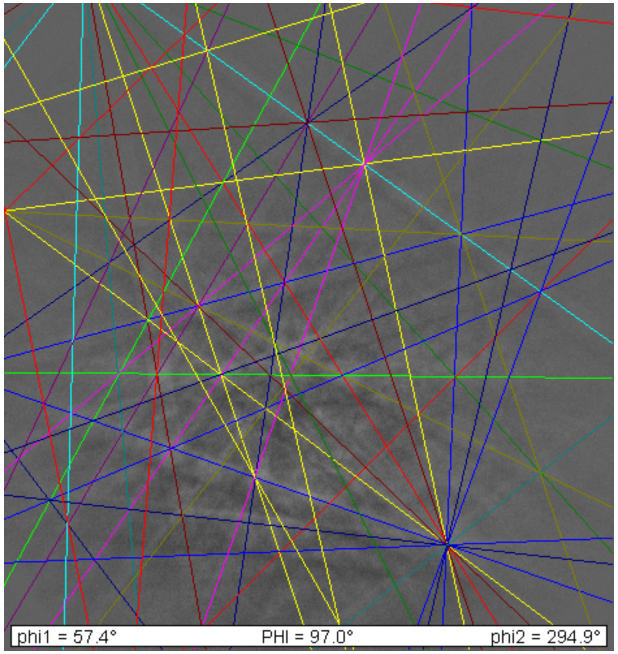

orthorhombic

S.G. 62 = Pbnm

Orientation map with confidence index

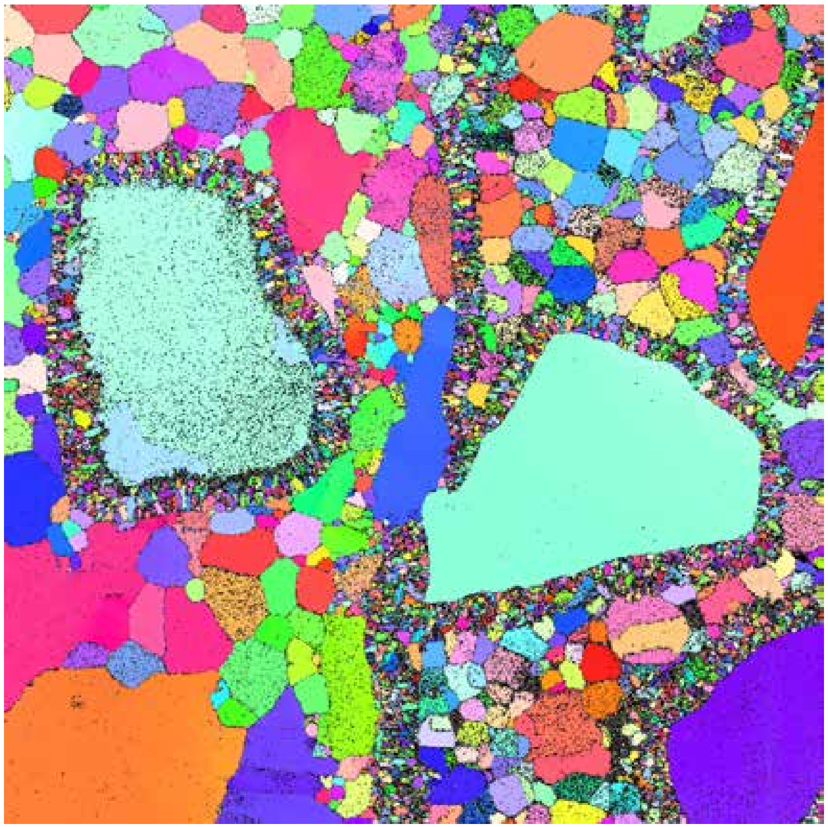

EBSD scan alone

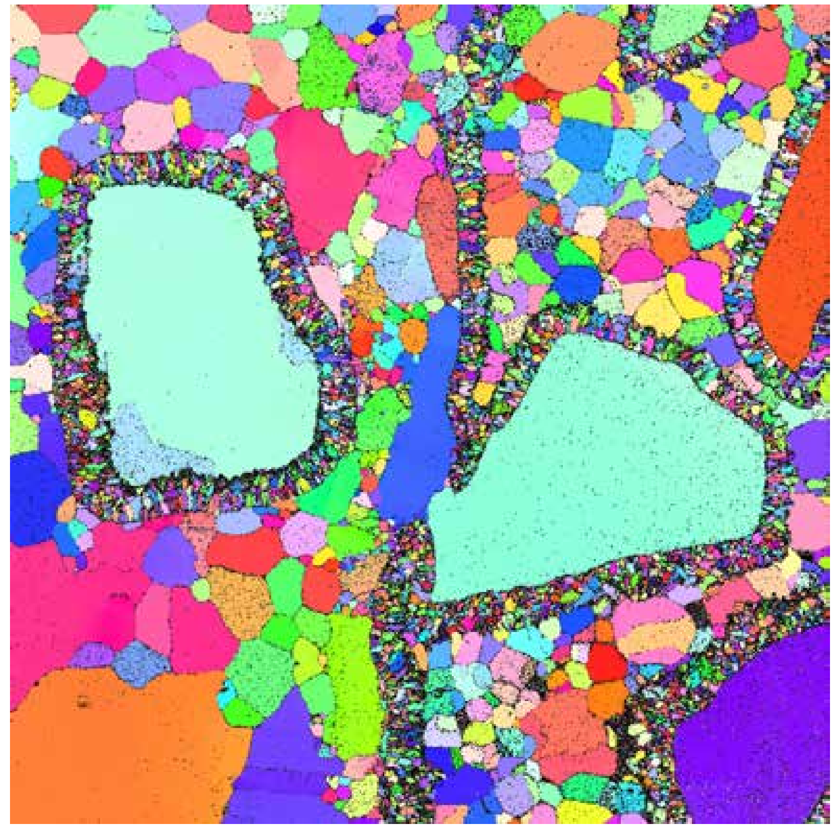

EBSD+EDS ChiScan

Element distributions

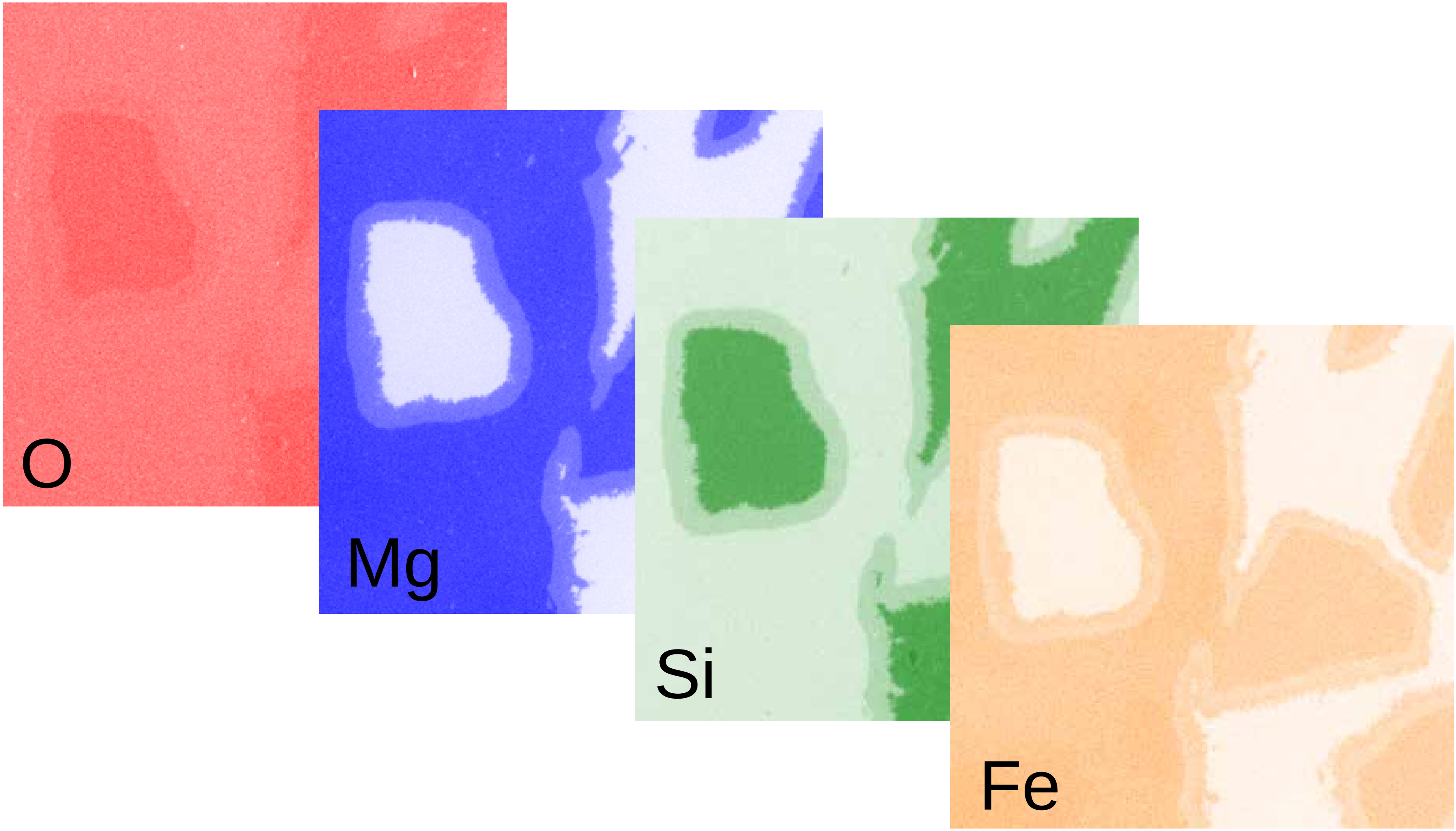

ChiScan: linking EDS into EBSD

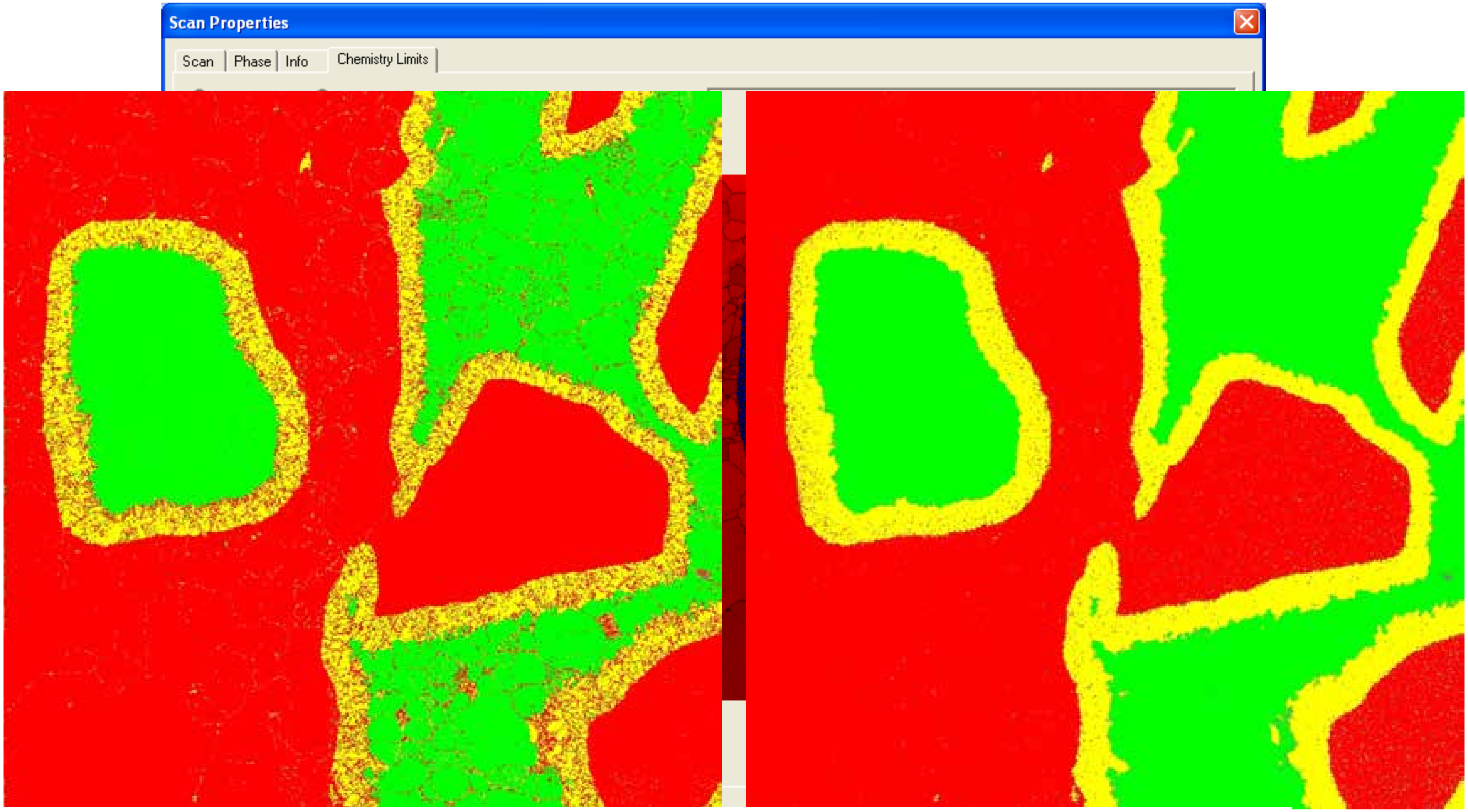

EBSD scan alone

ChiScan:
Phases filtered by EDX
Orientations by EBSD

Analytical SEM

1. Introduction

2. X-ray spectroscopy
   a) Emission of X-rays
   b) Detection of X-rays (EDX)
   c) Detection of X-rays (WDX)

3. Electron back scatter diffraction (EBSD)
   a) general basics
   b) recent developments

Ionisation of electron shells

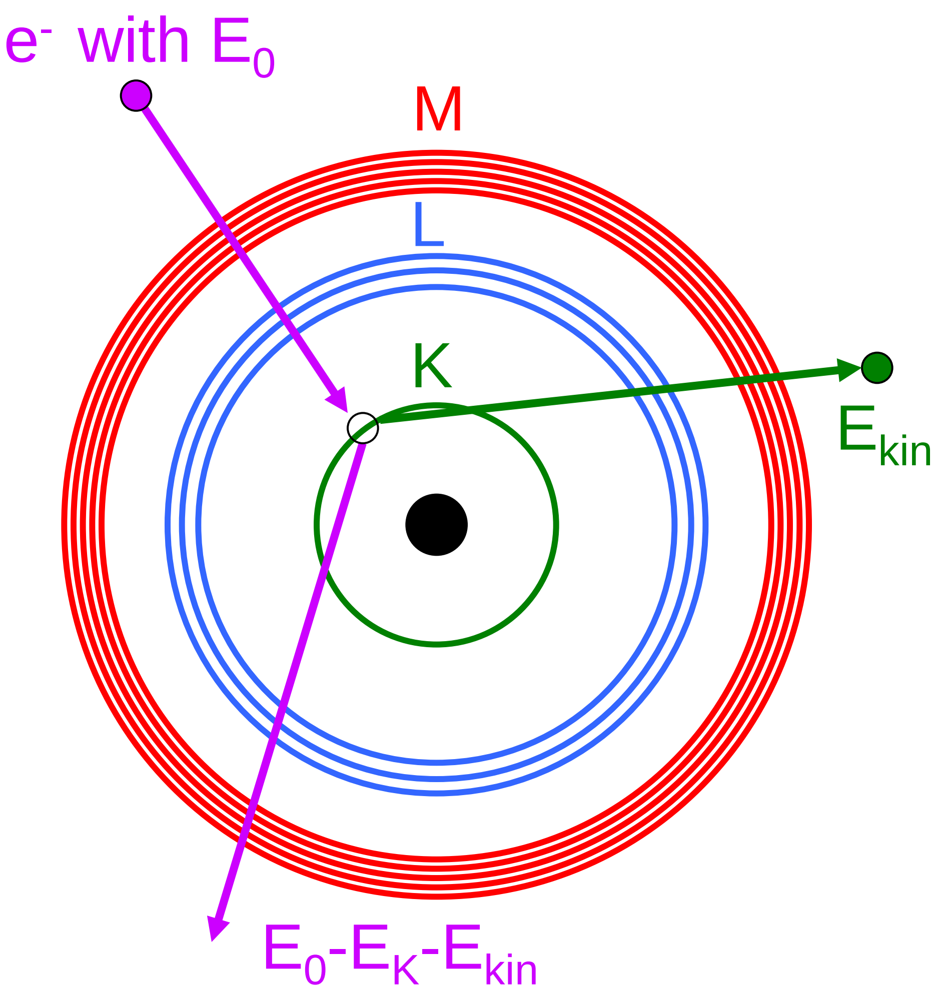

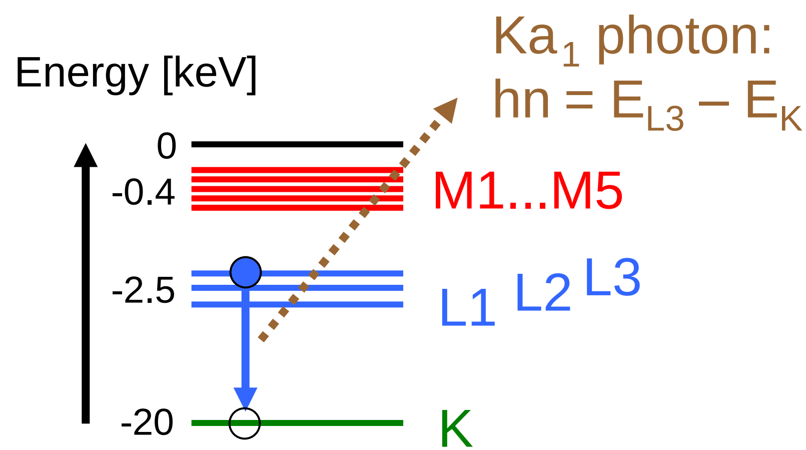

Term scheme
of Mo Atom

Per energy shell n:

2n-1 sub-shells
occupied with
$2n^2$ electrons in total

Moseley's law

$$h\upsilon_{K\alpha} = 13.6eV\ (Z-1)^2\left[\frac{1}{1^2}-\frac{1}{2^2}\right];$$

$$h\upsilon_{L\alpha} = 13.6eV\ (Z-7.4)^2\left[\frac{1}{2^2}-\frac{1}{3^2}\right]$$

Energy levels and characteristic X-ray lines for silver Z=47)

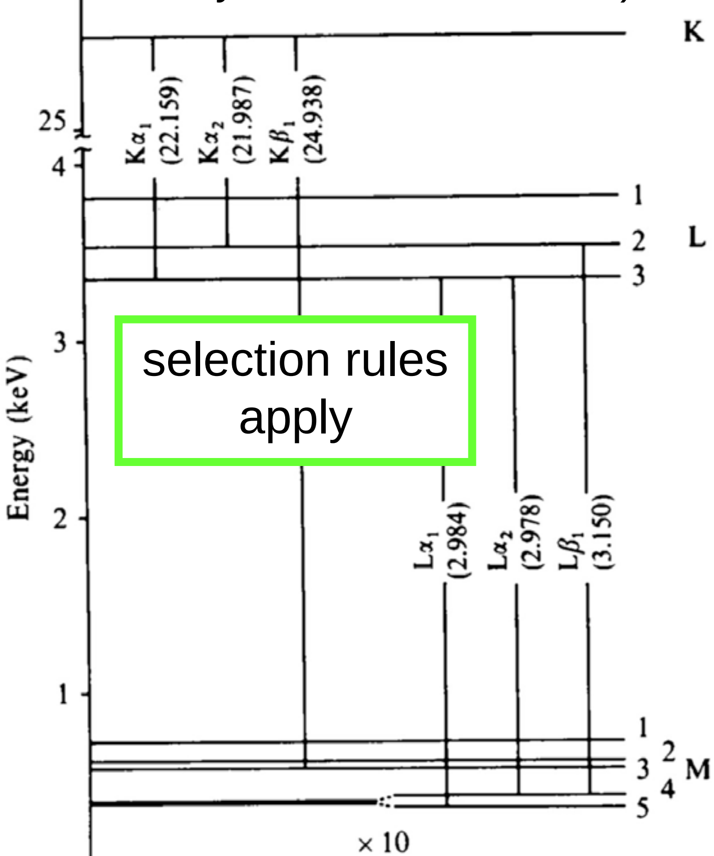

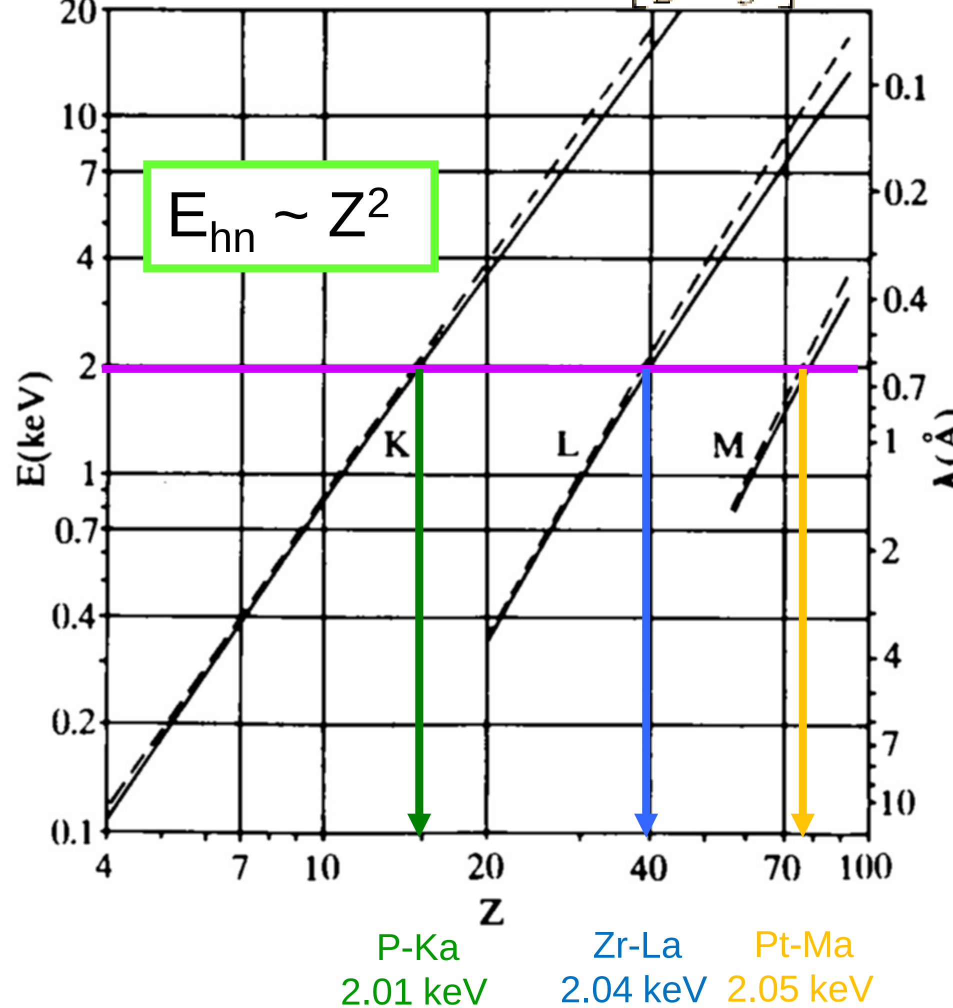

Characteristic X-ray lines

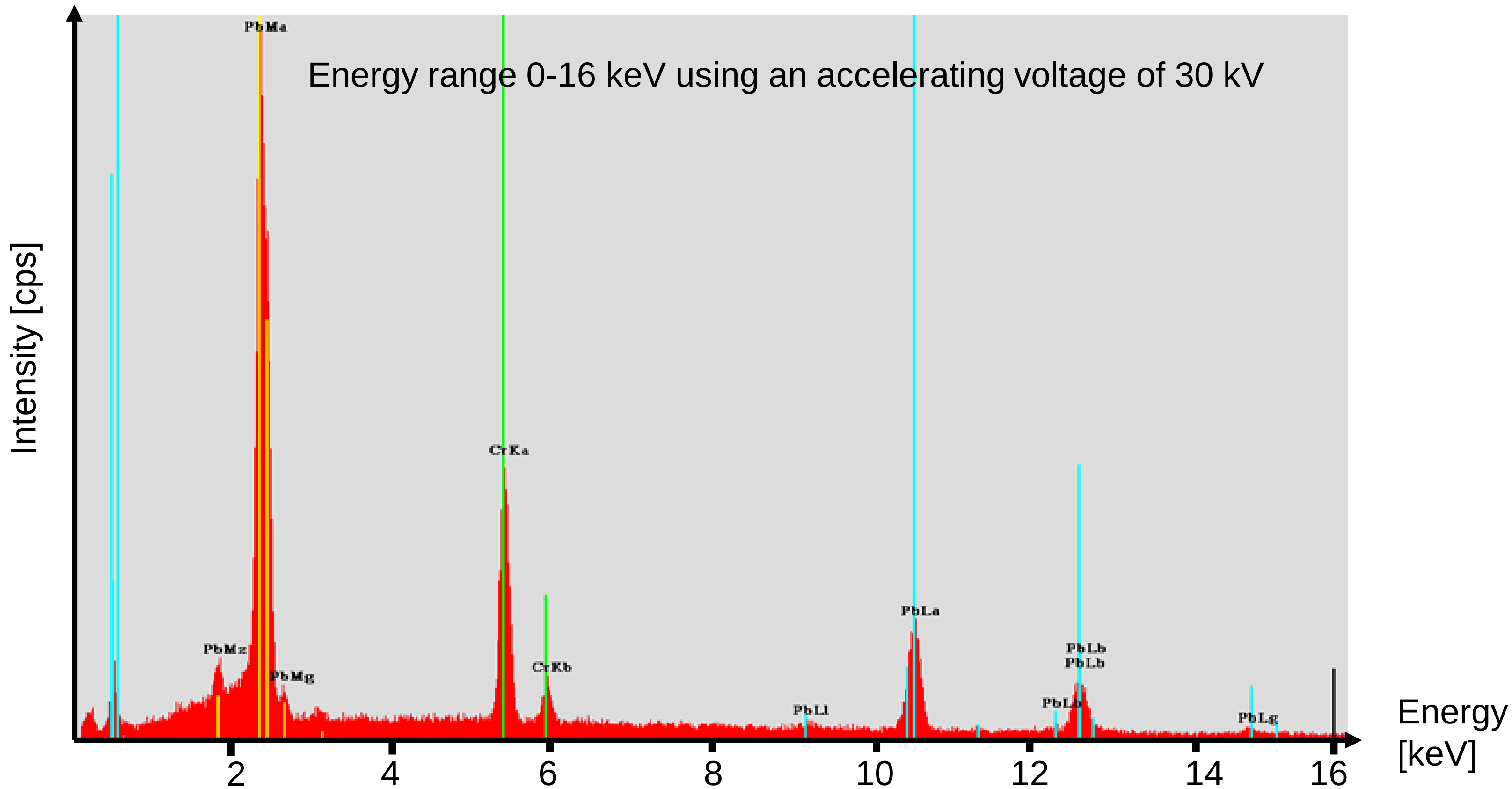

M - Lines:
Heavy elements
Z > 55 (Ba)

L - Lines:
Medium elements
Z > 31 (Ga) … Z < 80 (Hg)

K - Lines:
Light elements
Z < 40 (Zr)

ETH zürich

ScopeM

Characteristic lines – Moseley's law

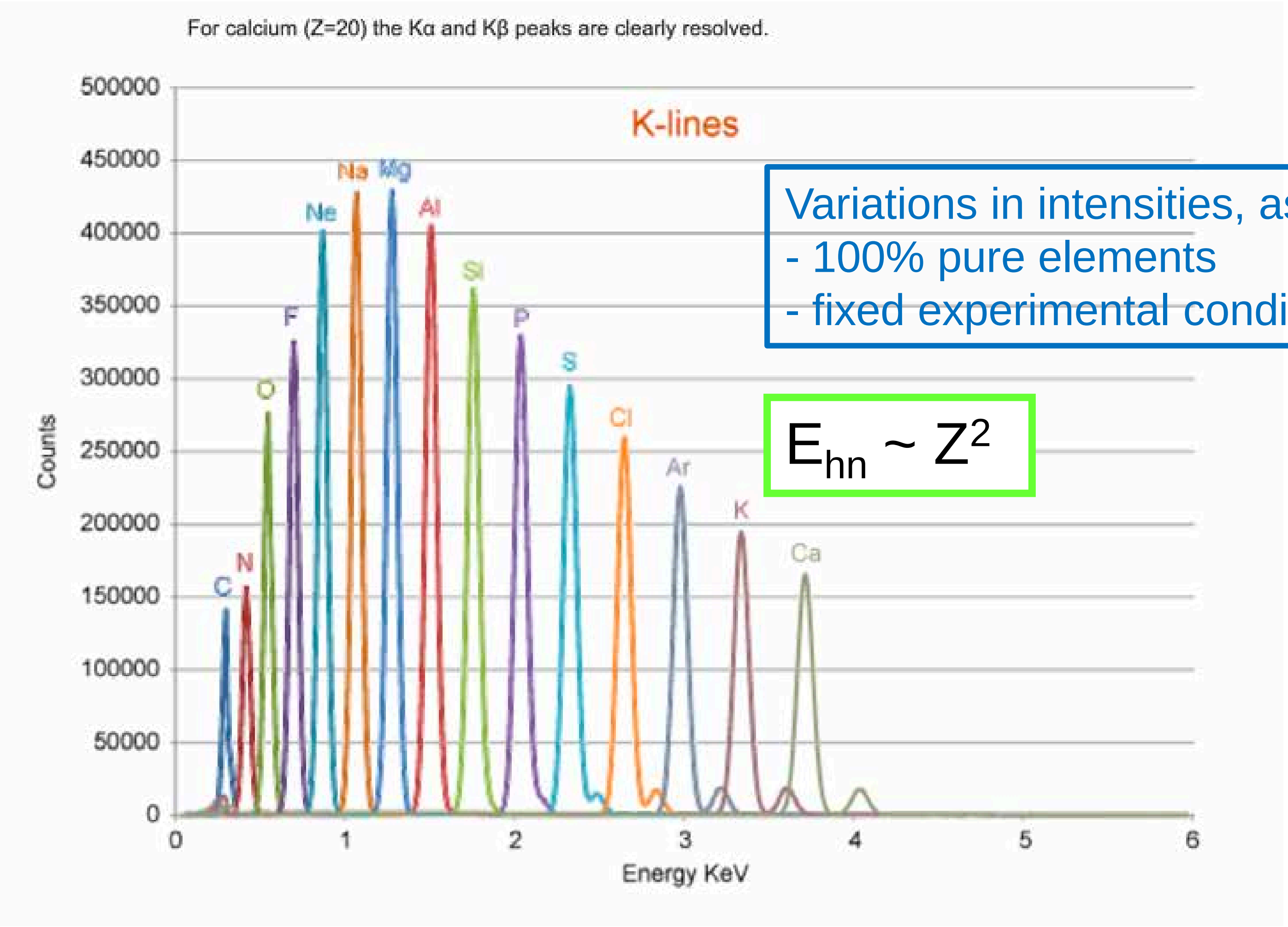

Variations in intensities, assuming
- 100% pure elements
- fixed experimental conditions

$E_{hn} \sim Z^2$

https://myscope.training/legacy/analysis/eds/xraygeneration/characteristic/#detail

Ionisation cross-section

- Q_K : Probability of K-shell ionisation
  - Overvoltage ratio
    $U = E_0 / E_K$
    E_0 = primary e-beam energy
    E_K = characteristic X-ray line
  - $\mathrm{sqrt}(Q_K) \sim 10^{-12}$ m
  - rapid decrease with Z

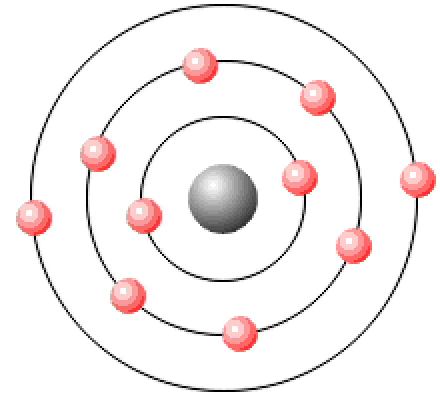

http://www.desy.de/pr-info/Roentgen-light/

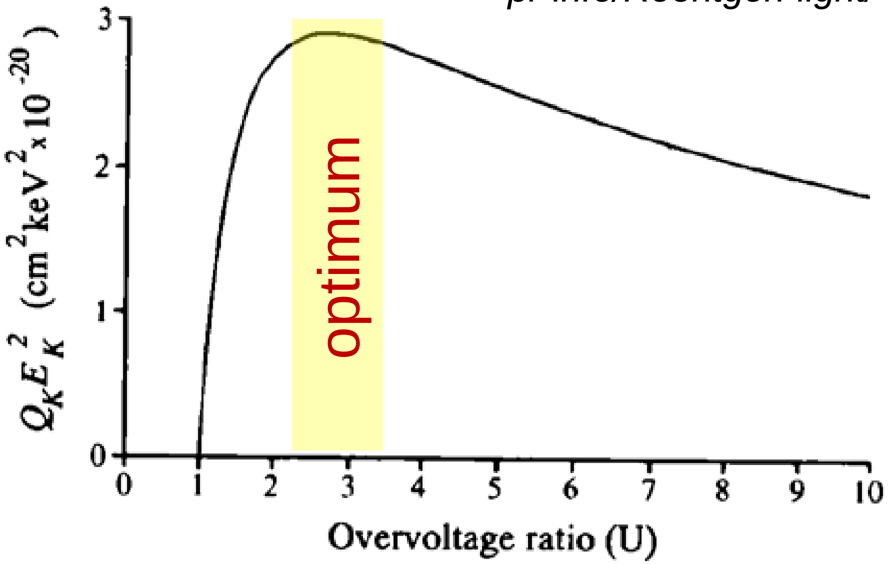

Energy release from excited state

- X-ray emission

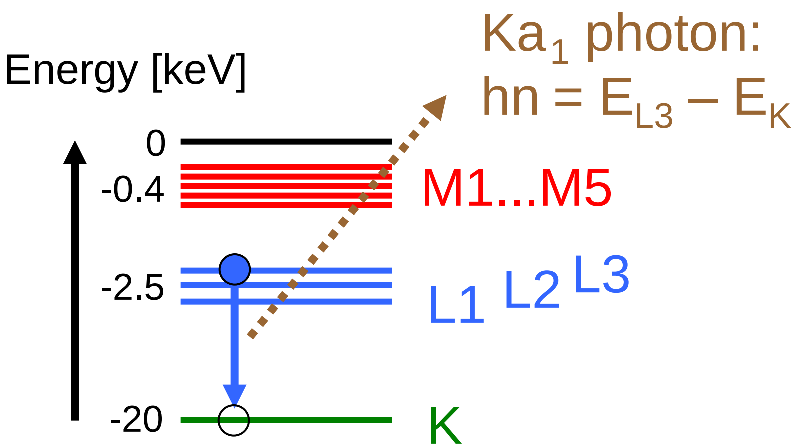

- Auger electron emission

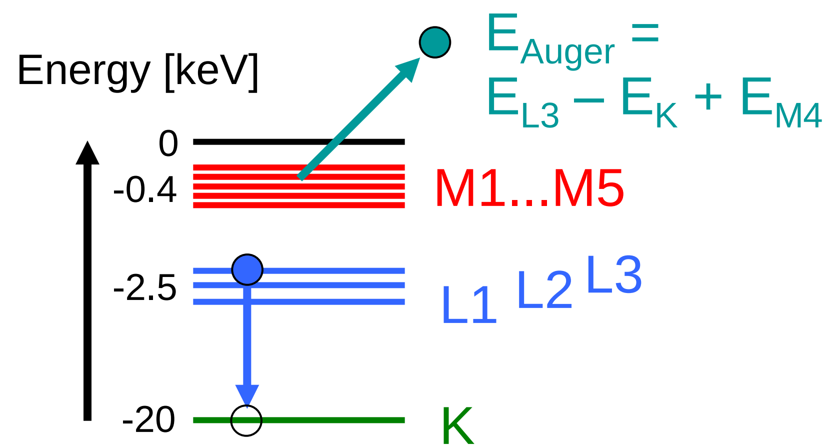

- Fluorescence yield
  - $w = Z^4 / (Z^4 + c)$
  - $c \sim 10^6$ for K-shell

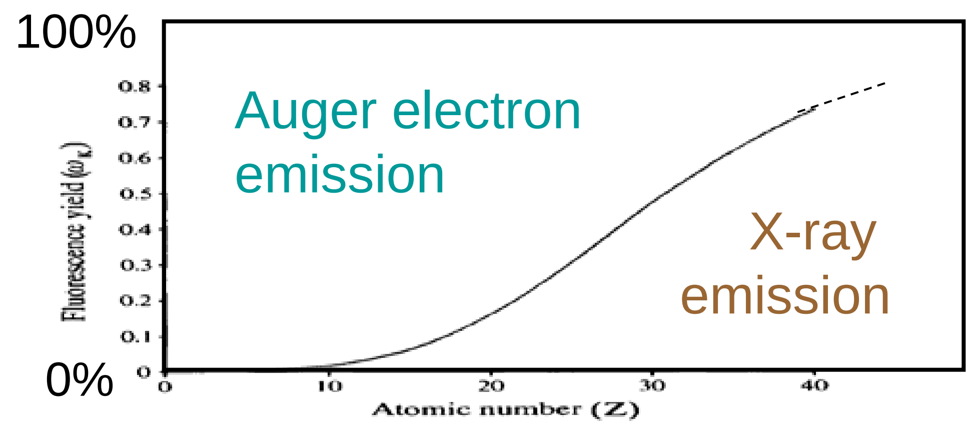

Bremsstrahlung

www.desy.de/pr-info/Roentgen-light/

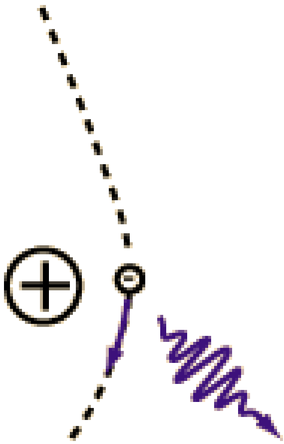

Accelerated electron emits radiation

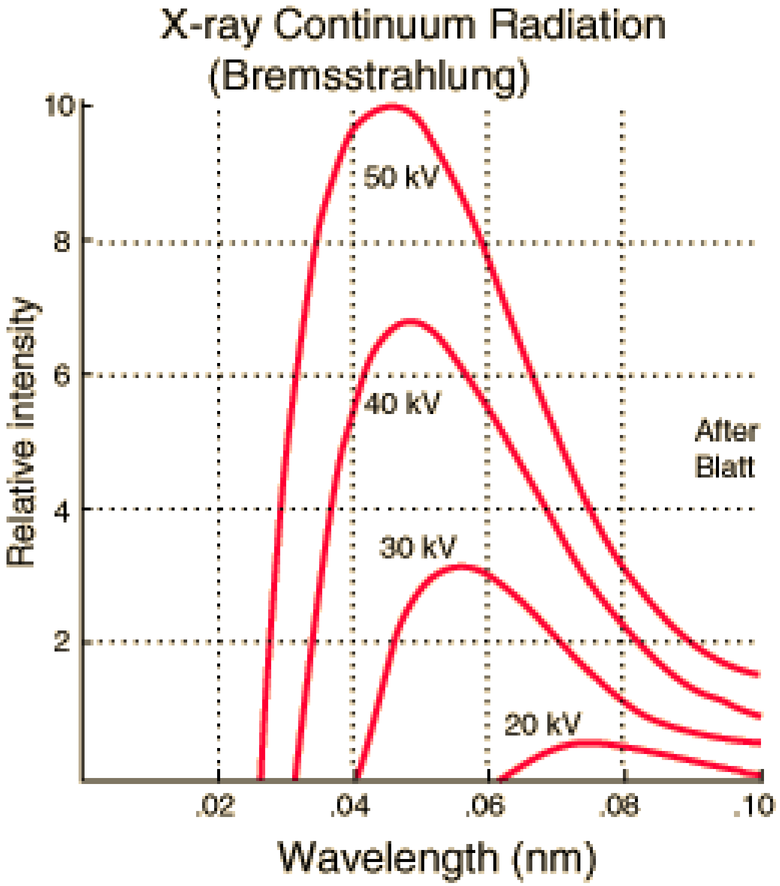

http://hyperphysics.phy-astr.gsu.edu/hbase/quantum/xrayc.html

X-ray spectra

- wavelength dispersive (WDX, WDS)

$N(l\ ) \sim Z\ (l\ - l_0) / (l_0 l^2)$

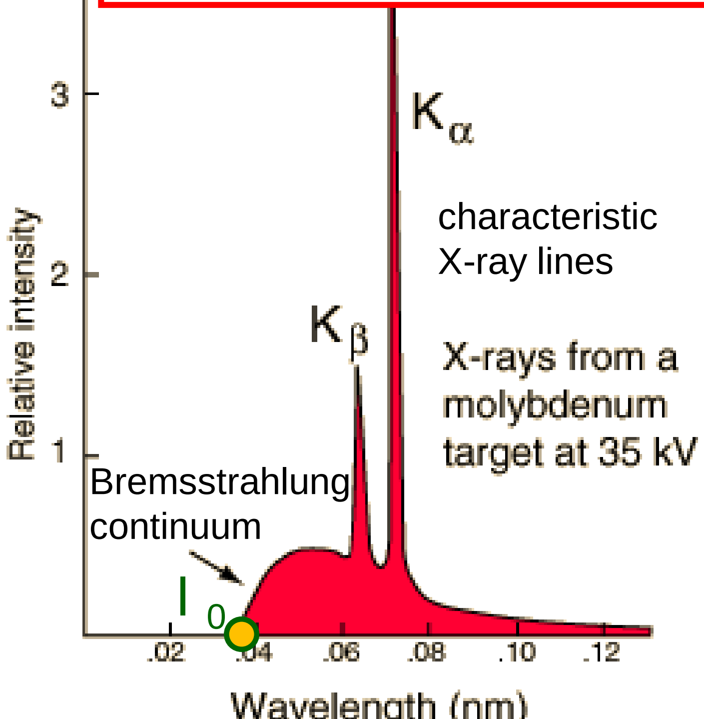

- energy dispersive (EDX, EDS)

$N(E) \sim Z\ (E_0 - E) / E$
(Kramers, 1923)

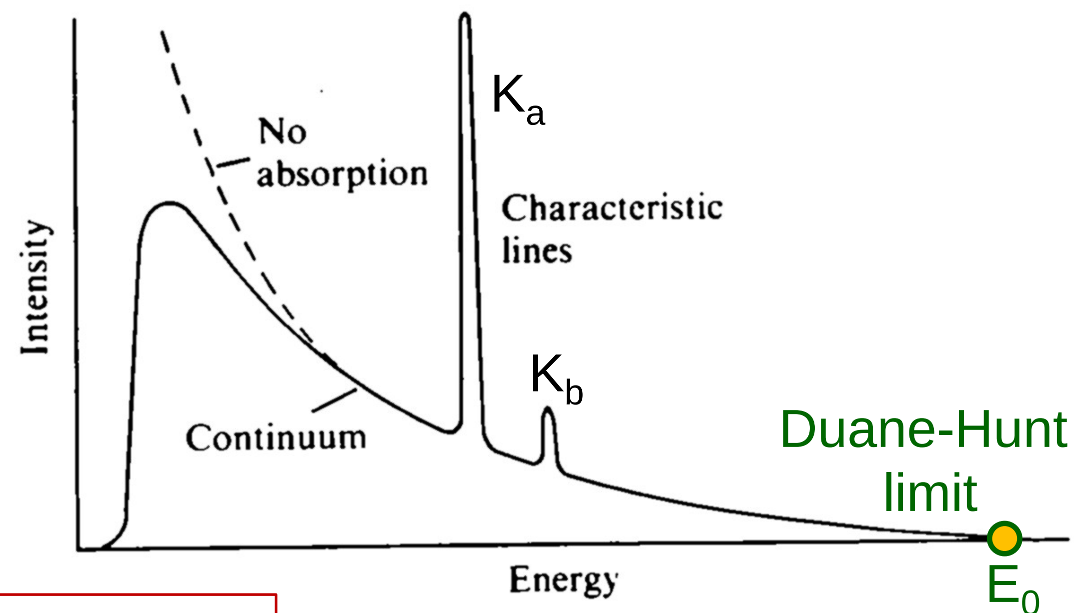

$El\ = hc$

Analytical SEM

1. Introduction

2. X-ray spectroscopy
   a) Emission of X-rays
   b) Detection of X-rays (EDX)
   c) Detection of X-rays (WDX)

3. Electron back scatter diffraction (EBSD)
   a) general basics
   b) modern trends

EDX: Semiconductor detector

fundamental principle

X-ray

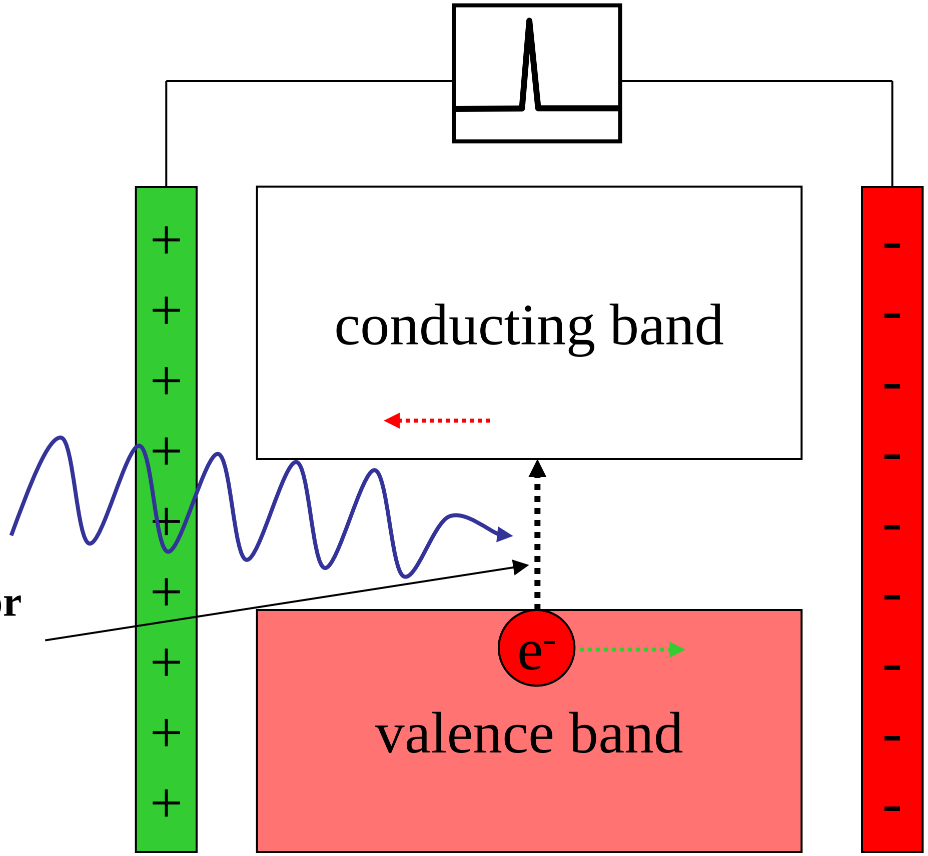

Creation energy for electron-hole pair
3.6 eV for Si
2.9 eV for Ge

Band gap
1.1 eV for Si
0.67 eV for Ge

number of e^- transferred μ energy of photon

p-i-n junction

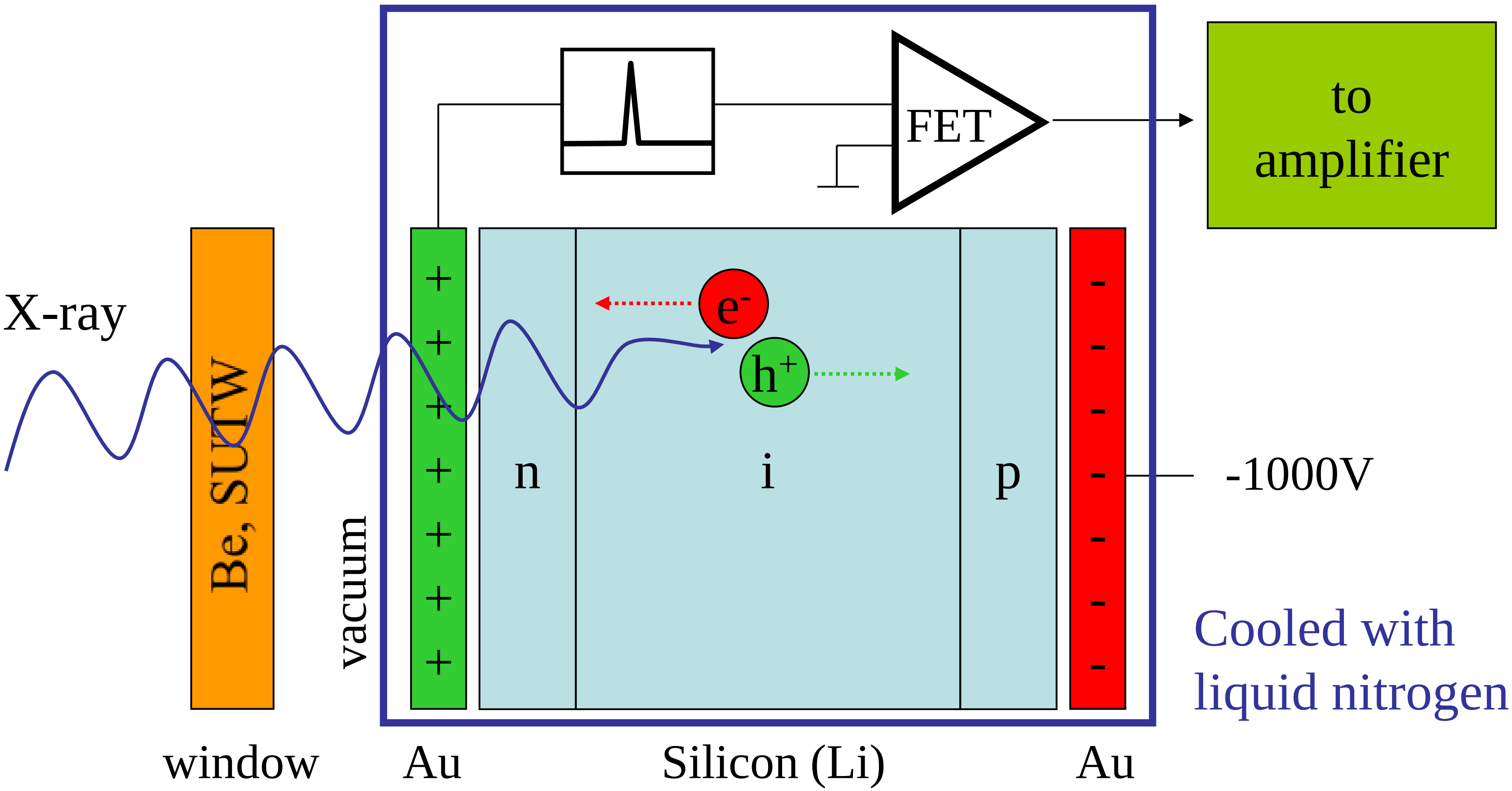

reverse bias Þ no current due to applied voltage

Why to cool EDS detector?

- Thermal activation induces electron-hole pair generation, giving noise that handicaps detection of an X-ray signal.

- The Li-atoms would diffuse under applied bias, destroying the intrinsic region of the detector.

- The electronic noise of the FET could mask signals from low-energy X-rays.

Detector cooling and window

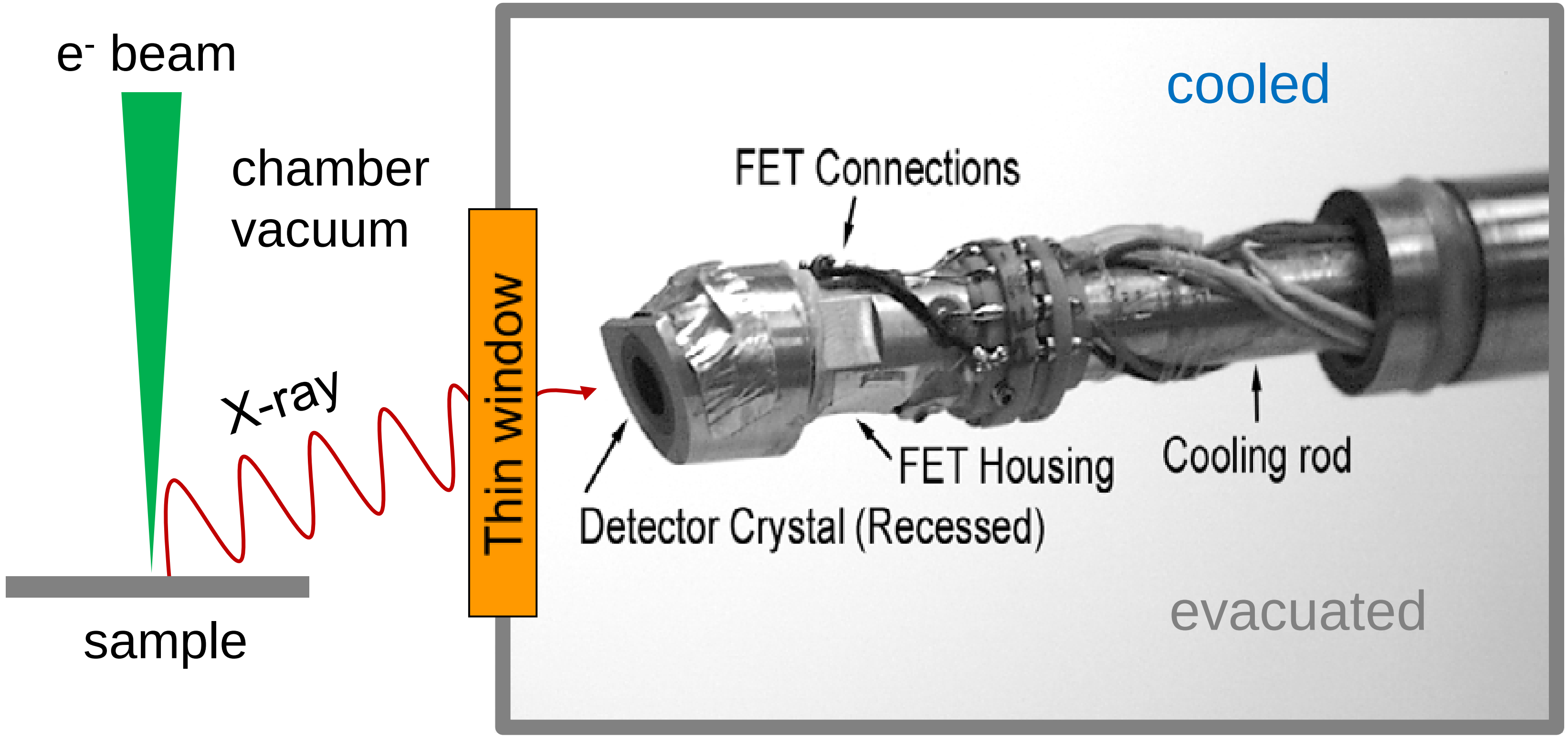

Cold surfaces attract frost formation:

- No problem, as long as good vacuum is maintained (windowless systems)
- Major issue, when chamber vacuum is broken (SEM chamber vent, leakage)

Absorption by detector window

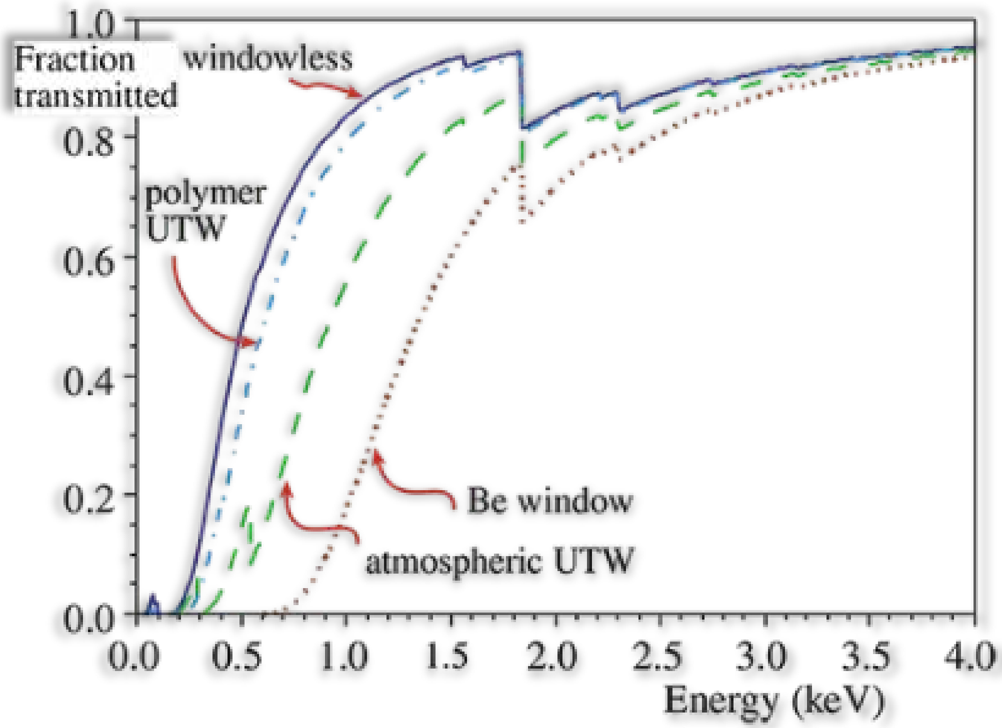

- Limitation particularly for low-energy (light element) X-ray detection
- Technology steps towards thinner windows of lighter materials:

  Be à UTW à SUTW à SiN_x à windowless

Schematic: Transmission Electron Microscopy. Williams & Carter 2009

EDX detector Si(Li) on SEM

Connection to liquid nitrogen level sensor

Liquid nitrogen tank

Retraction mechanics and pre-amplifier

Detector

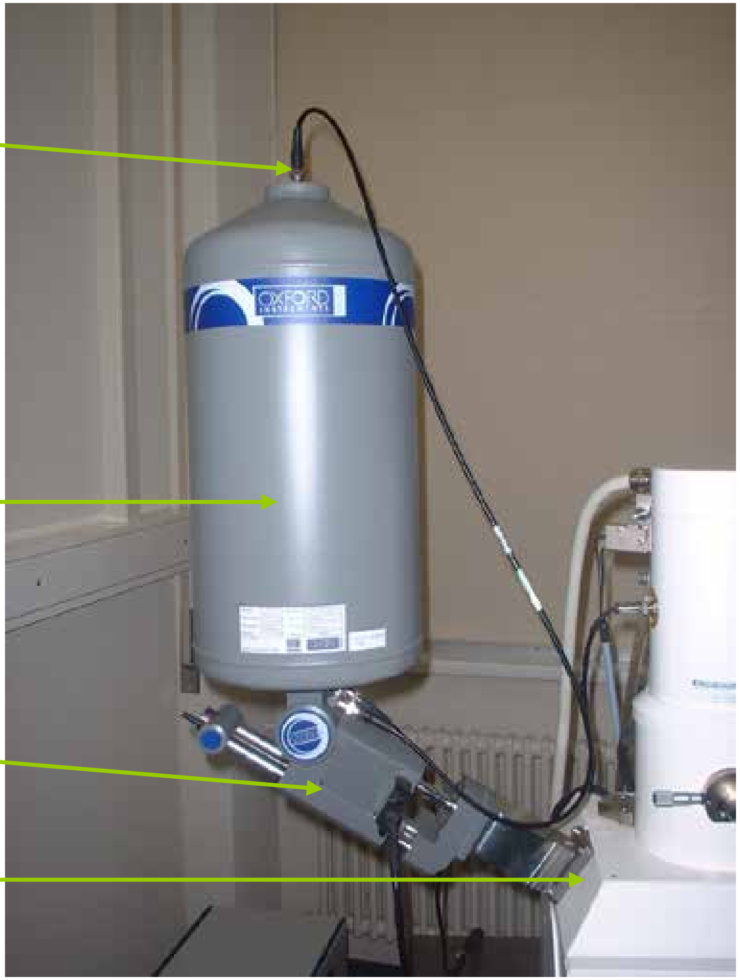

EDX detector Si(Li) on TEM

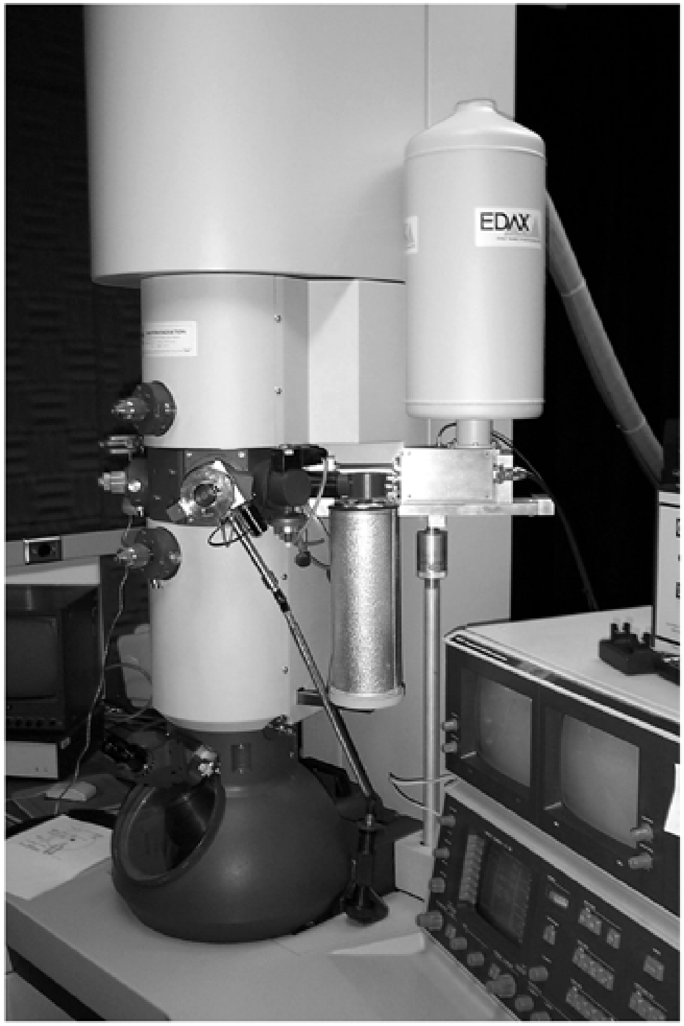

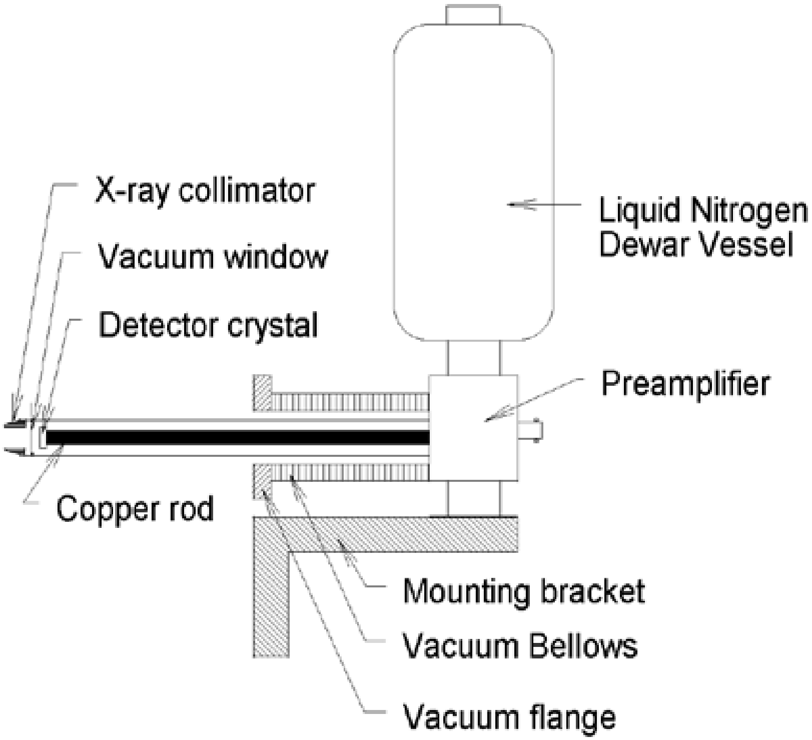

- Protective measures in case of over-exposure:
  - Motorized retraction
  - Shutter mechanism

Si(Li) vs SDD

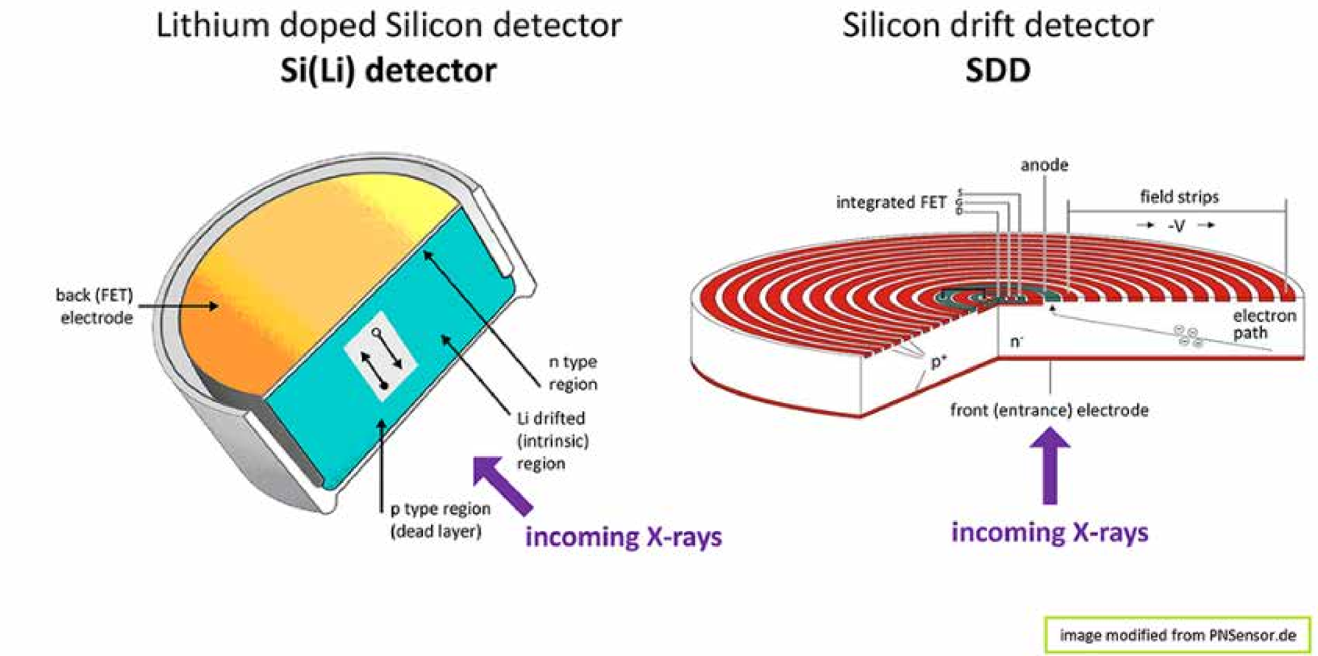

Same fundamental principle, but different geometrical design:

- Applying voltage from inside to outside the detector (rather than front to back as in Si(Li)) permits collection of the electrons in the n-Si with 4 times lower voltage.
- The central anode in the middle of p-doped rings has much smaller capacitance than the large rear face anode of Si(Li), allowing for much higher throughput of counts.

Benefits:
- Peltier cooling sufficient
- energy resolution rather independent on count rates
- highest count rates (> 1 Mcps input)

ChemiSTEM^{TM}: 'hours to minutes'

STEM-EDX at 200kV

www.fei.com

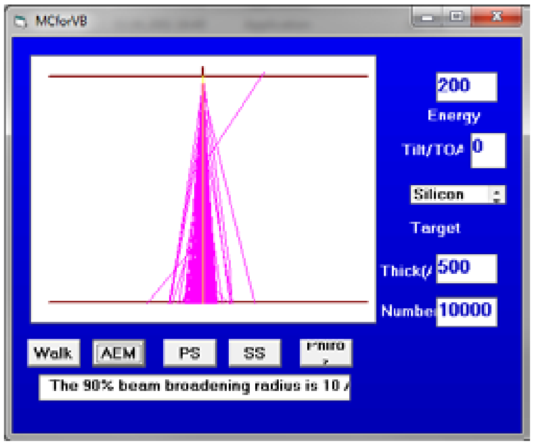

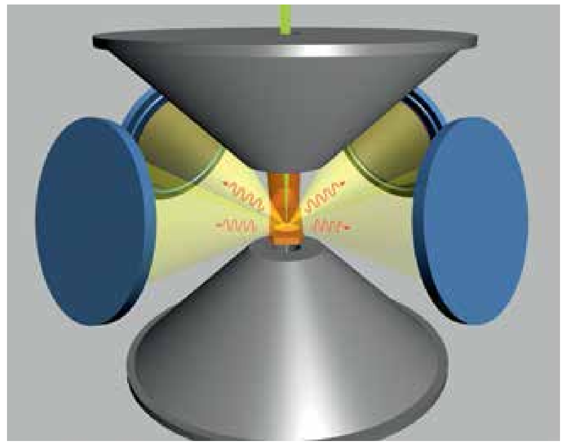

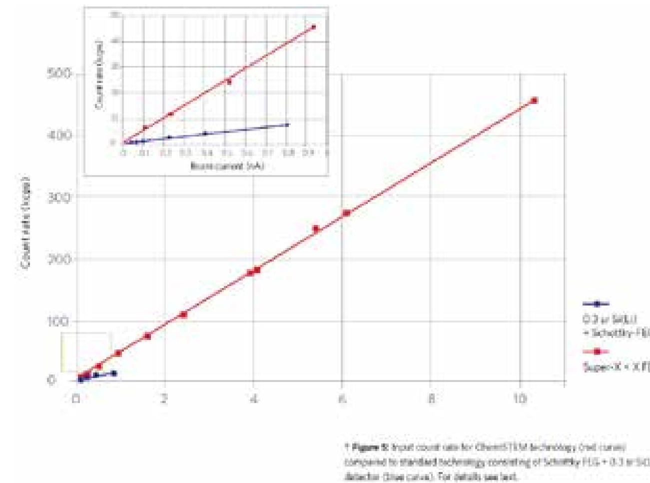

- High brightness X-FEG
  - à 5x more X-ray generation
- Super-X with 4 SDD
  - à total solid angle 0.9 sr
  - à windowless design
  - à 5-10x more X-ray collection

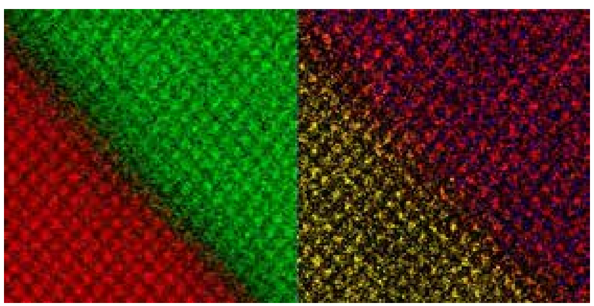

Atomic resolution chemical map
of $GdScO_3/SrTiO_3$ interface showing the elemental distribution of Sc and Ti. The EELS signal (left) and the EDS signal (right) is simultaneously acquired with 500sp/s and 256x256 pixel (total acquisition time: 2 minutes)
Sample courtesy: Dr. M. Luysberg, Ernst Ruska Centrum, Germany

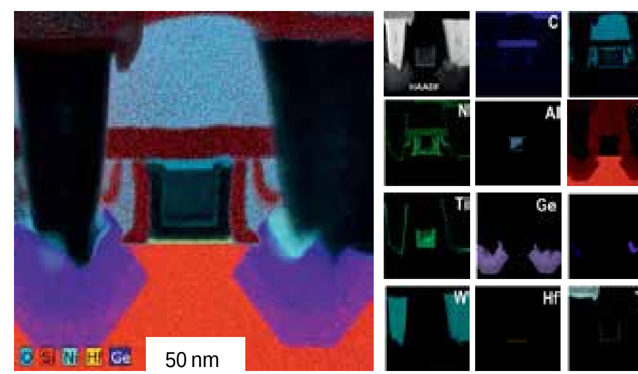

Large Maps, All Elements
600 x 600 pixel maps of a 45 nm PMOS transistor structure recorded with 50 µsec dwell time/pixel and 1 nA beam current. Drift correction was applied to acquire multiple frames in 100 minutes. The maps were fully quantified to eliminate contributions from overlapping peaks. (Pixel size 0.3 nm)
Data courtesy by D. Klenov, FEI

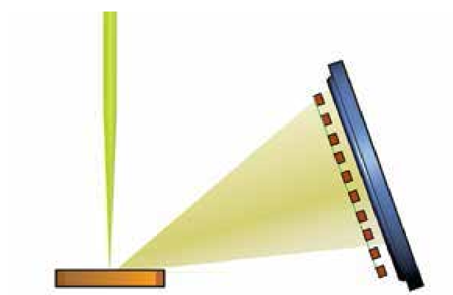

Conventional STEM-EDX

ETH zürich   ScopeM

EDX – further topics – not covered

- Interaction volume (vs. Z and kV)
- Spectral resolution (fundamental limit)
- Peak overlaps
- Spectrum artifacts (pile-up, escape, stray)
- (Semi-) quantitative analysis
- Hyperspectral (element & phase) mapping
- …

NEW: EDX imaging detectors

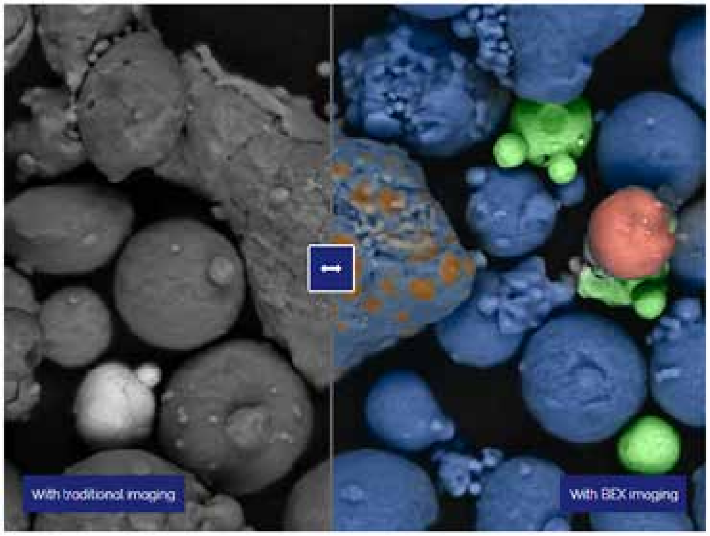

Unity Detector - Nanoanalysis - Oxford Instruments

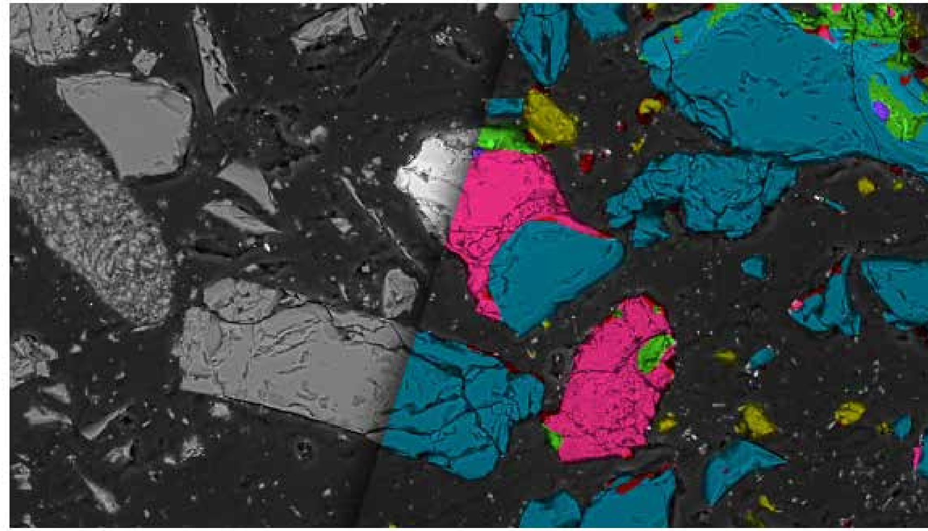

ChemiPhase image of a refractory material (brown fused alumina) employed in steel production. The phase analysis shows the location of the alumina (light blue) but also the presence of unexpected materials that act as contamination, such as titanium oxide (displayed in pink) and fragments of silica (displayed in yellow)

SEM EDS | SEM EDX | ChemiSEM Technology | Thermo Fisher Scientific - CH

- UI software integration
  of SEM imaging and EDX signals

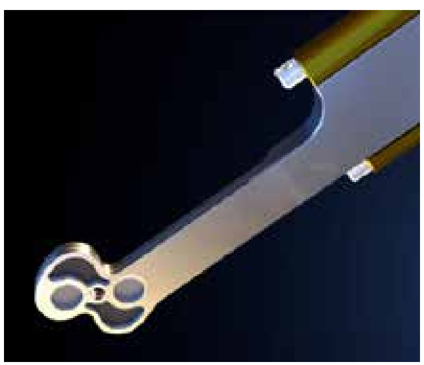

- Flat design of BSE + EDX detector segments
- Large collection angle and sensitivity

à Element mapping in imaging speed

Analytical SEM

1. Introduction

2. X-ray spectroscopy
   a) Emission of X-rays
   b) Detection of X-rays (EDX)
   c) Detection of X-rays (WDX)

3. Electron back scatter diffraction (EBSD)
   a) general basics
   b) recent developments

Spectral resolution: EDS vs. WDS

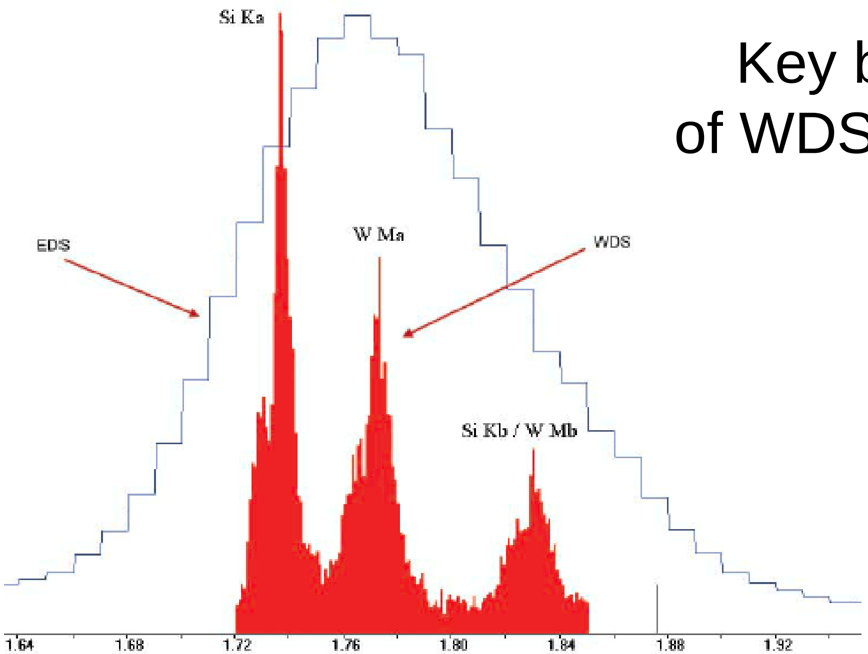

Si-W sample showing excellent separation of Si Kα and W Mα peaks

Key benefit of WDS systems

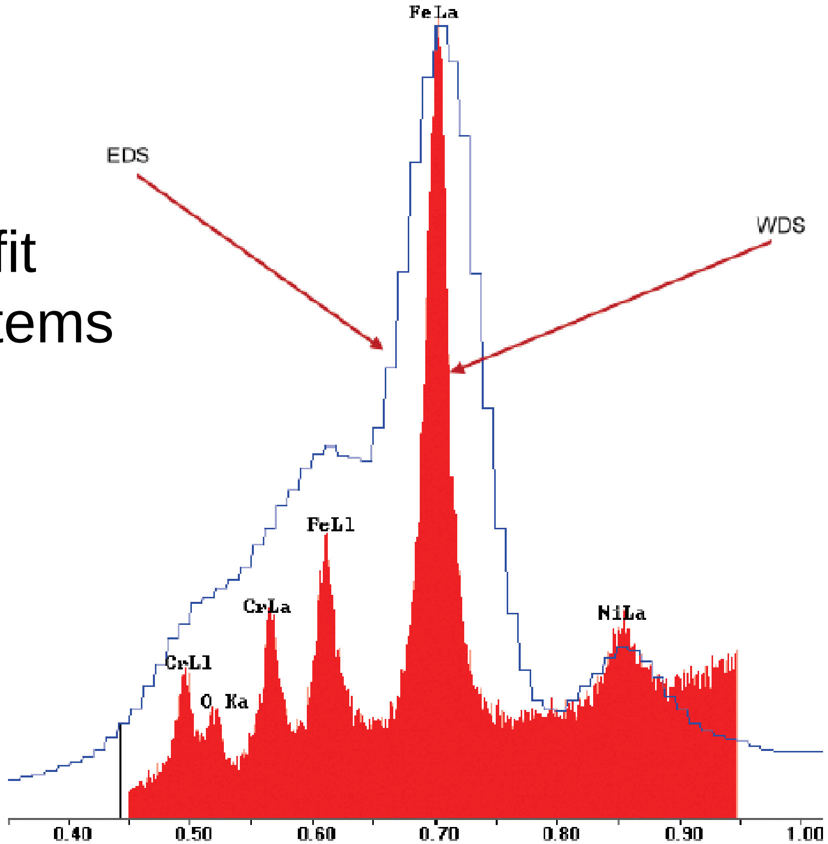

Transition Elements - L lines

Focusing WDX spectrometer

Spectrometer

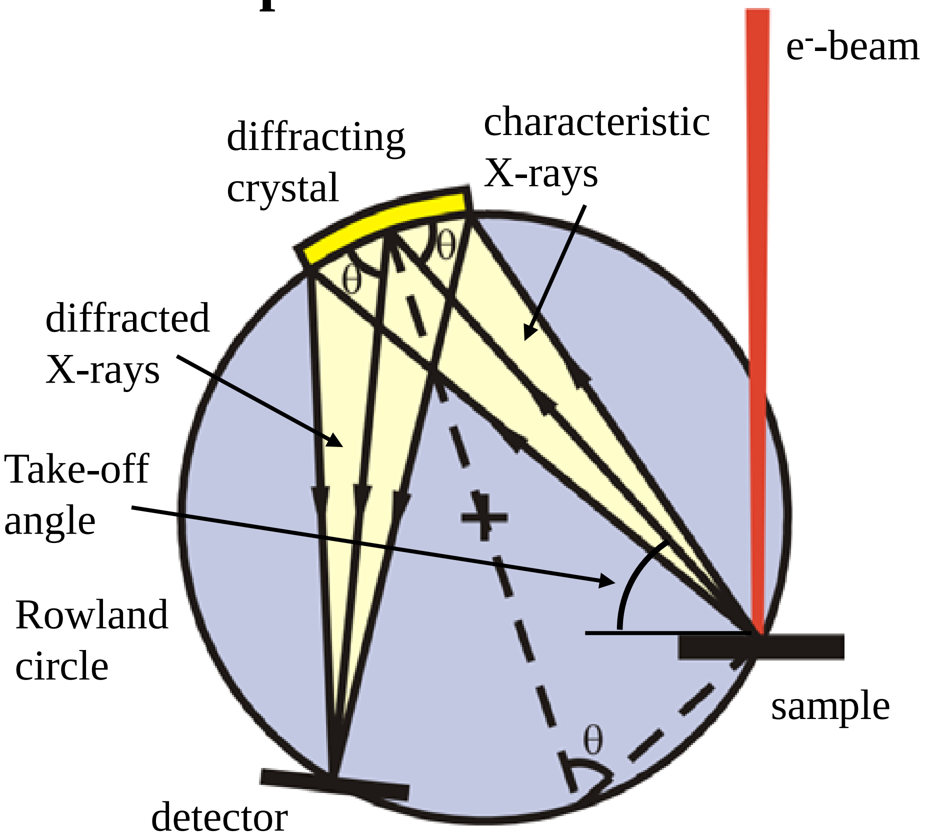

Diffracting crystal

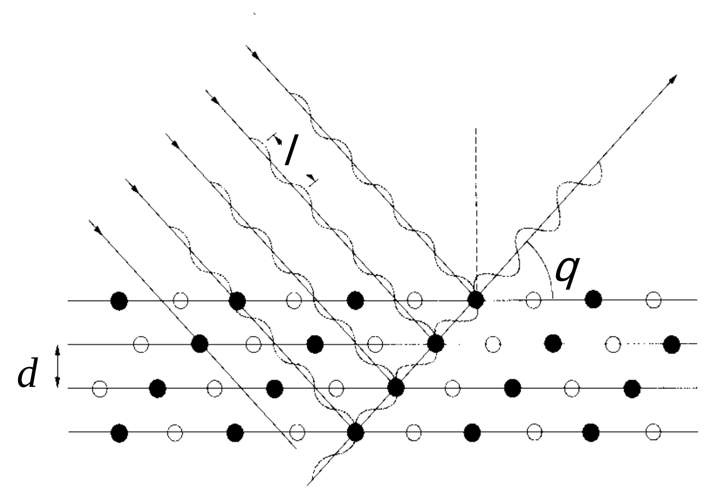

Bragg's Law

$$n \cdot \lambda = 2d \cdot \sin(\theta)$$

WDX analysis

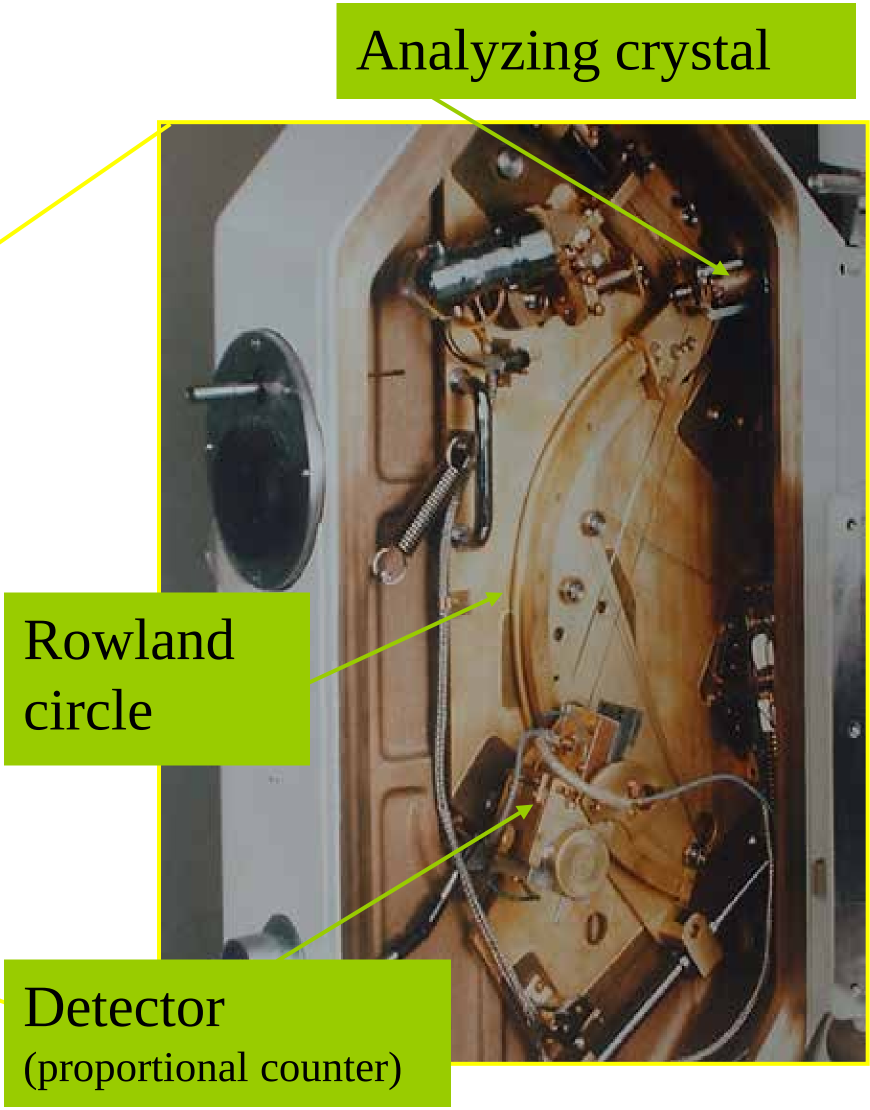

Parallel Beam X-ray Spectrometer

- Single detector design for usage at SEM
- simultaneous analysis by WDX and EDX detectors

www.thermoscientific.com

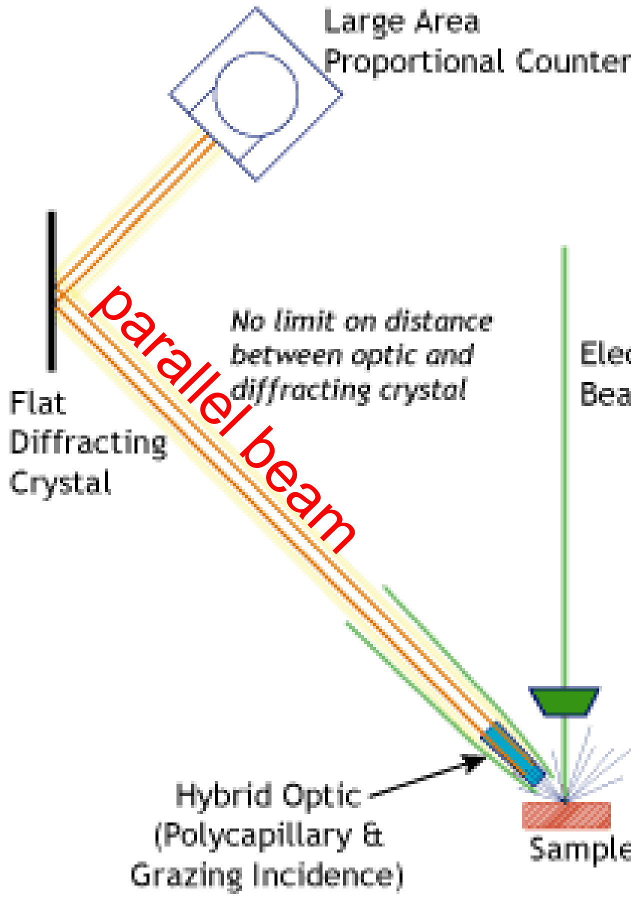

www.edax.com

Comparison

$E\lambda = hc$

EDX

+ Fast measurement
  - About 1 minute measuring time for a whole spectrum
- Low energy resolution
  - 120 – 150 eV
- Higher detection limit
  - parts of %
- Lower count rates
  - (negative influence on detection limit and accuracy)
- No mechanical parts

WDX

- Long measuring time
  - About 10 minutes for a coarse qualitative spectrum
+ High spectral resolution
  - about 10 eV
+ Low detection limit
  - down to 100 ppm
+ High count rates
- Mechanical spectrometer
  - Stable environment, wear

Comparison of X-ray spectrometers

Characteristic	IG	Si(Li)	SDD	WDS
Energy resolution (typical/on column)	135 eV	150 eV	140 eV	10 eV
Energy resolution (best)	114 eV	128 eV	127 eV	5 eV
Energy to form electron-hole pairs (77 K)	2.9 eV	3.8 eV	3.8 eV	n.a.
Band gap energy (indirect)	0.67 eV	1.1 eV	1.1 eV	n.a.
Cooling required	LN_2 or thermoelectric	LN_2/thermoelectric	None/ thermoelectric	None
Detector active area	10–≥50 mm^2	10–≥50 mm^2	≥50 mm^2	n.a.
Detector arrays available	No	No	Yes	No
Typical output rates	5–10 kcps	5–20 kcps	1000 kcps	50 kcps
Time to collect full spectrum	~1 min	~1 min	few secs	~30 min
Collection angle (sr)	0.03–0.20	0.03–0.30	0.3	10^{-4}–10^{-3}
Take-off angle	0°/20°/72°	0°/20°/72°	20°	40°–60°
Artifacts	Escape, sum peaks Ge K/L peaks	Escape, sum peaks Si K peak	Multiple sum peaks	High-order lines

TABLE 32. 2. Comparison of X-ray Spectrometers

Data in this table come from the Web sites of the leading XEDS manufactures. For the latest information, check the URLs listed in the reference section.

Table: Transmission Electron Microscopy. Williams & Carter 2009

Analytical SEM

1. Introduction

2. X-ray spectroscopy
   a) Emission of X-rays
   b) Detection of X-rays (EDX)
   c) Detection of X-rays (WDX)

3. Electron back scatter diffraction (EBSD)
   a) general basics
   b) recent developments

Electron backscatter (Kikuchi) diffraction

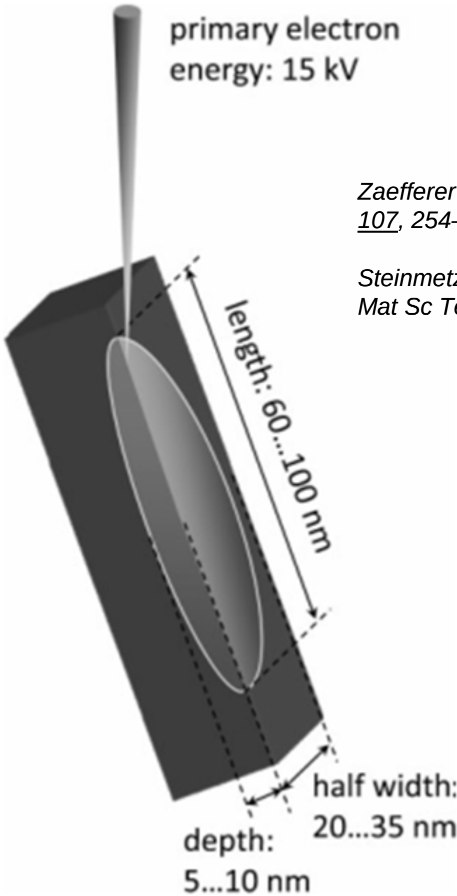

Zaefferer (2007) Ultramicroscopy, 107, 254–266

Steinmetz & Zaefferer (2010) Mat Sc Techn 26, 640-645

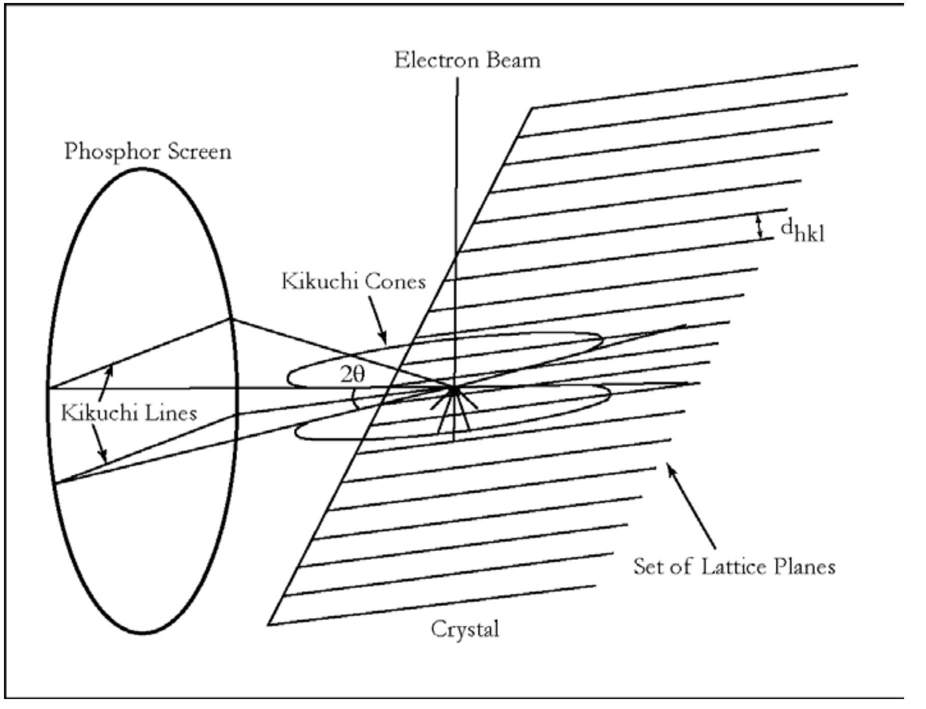

- Multiple interaction in bulk (thick) sample
- Diffuse scattering with loss of phase
- Interference of backscattered electrons
- Geometry follows Bragg diffraction

Kinematic theory

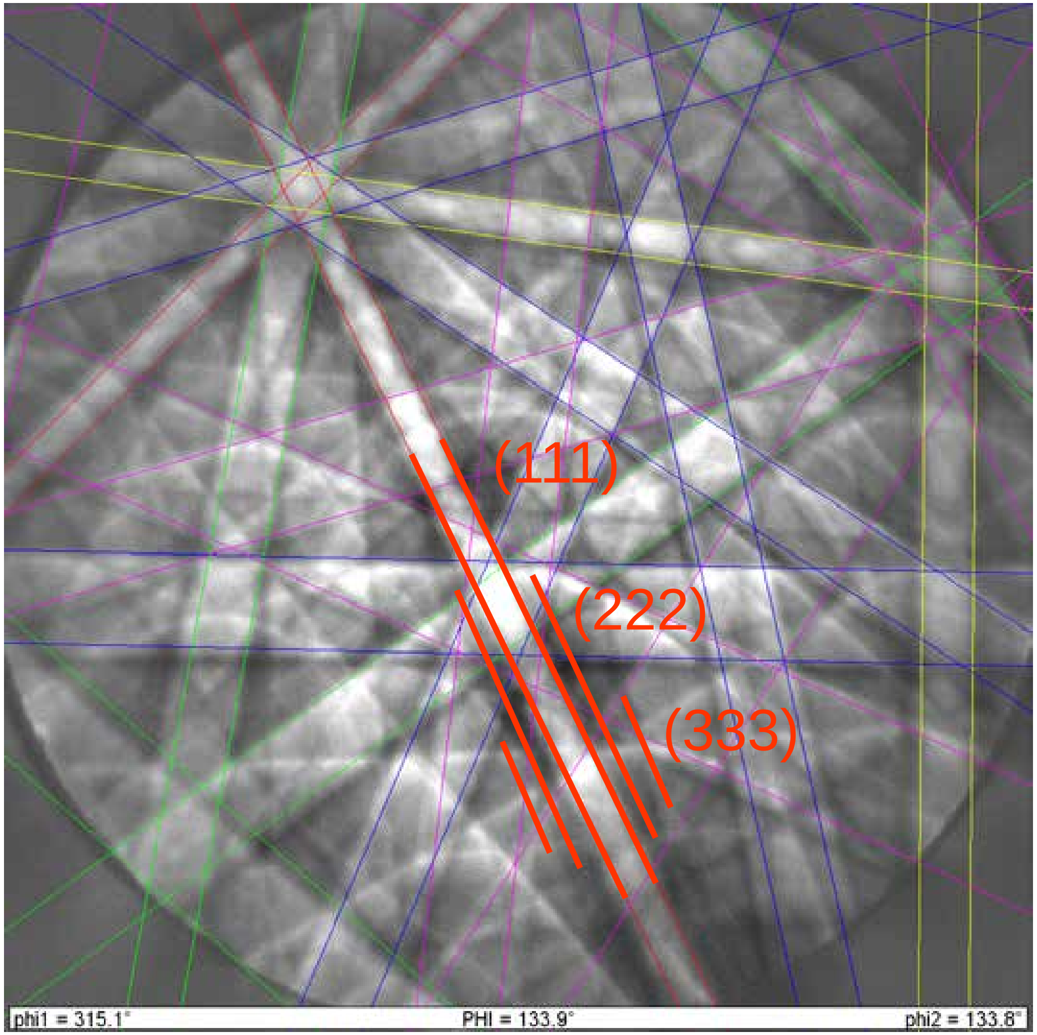

Nickel (fcc) 20 kV

$$2 d \sin Q = n l$$

(hkl)	d	2Q
(111)	2.032 Å	2.82°
(200)	1.760 Å	3.26°
(220)	1.245 Å	4.62°
(311)	1.061 Å	5.40°
(420)	0.787 Å	7.35°

- band width
  ~ 1 / lattice spacing
- band contrast
  ~ structure amplitude
- Interactive intensity corrections or based on two-beam dynamical theory

(Zaefferer (2007) Ultramicroscopy 107, 254–266)

ETH zürich Scope M

Indexing of EBSD pattern

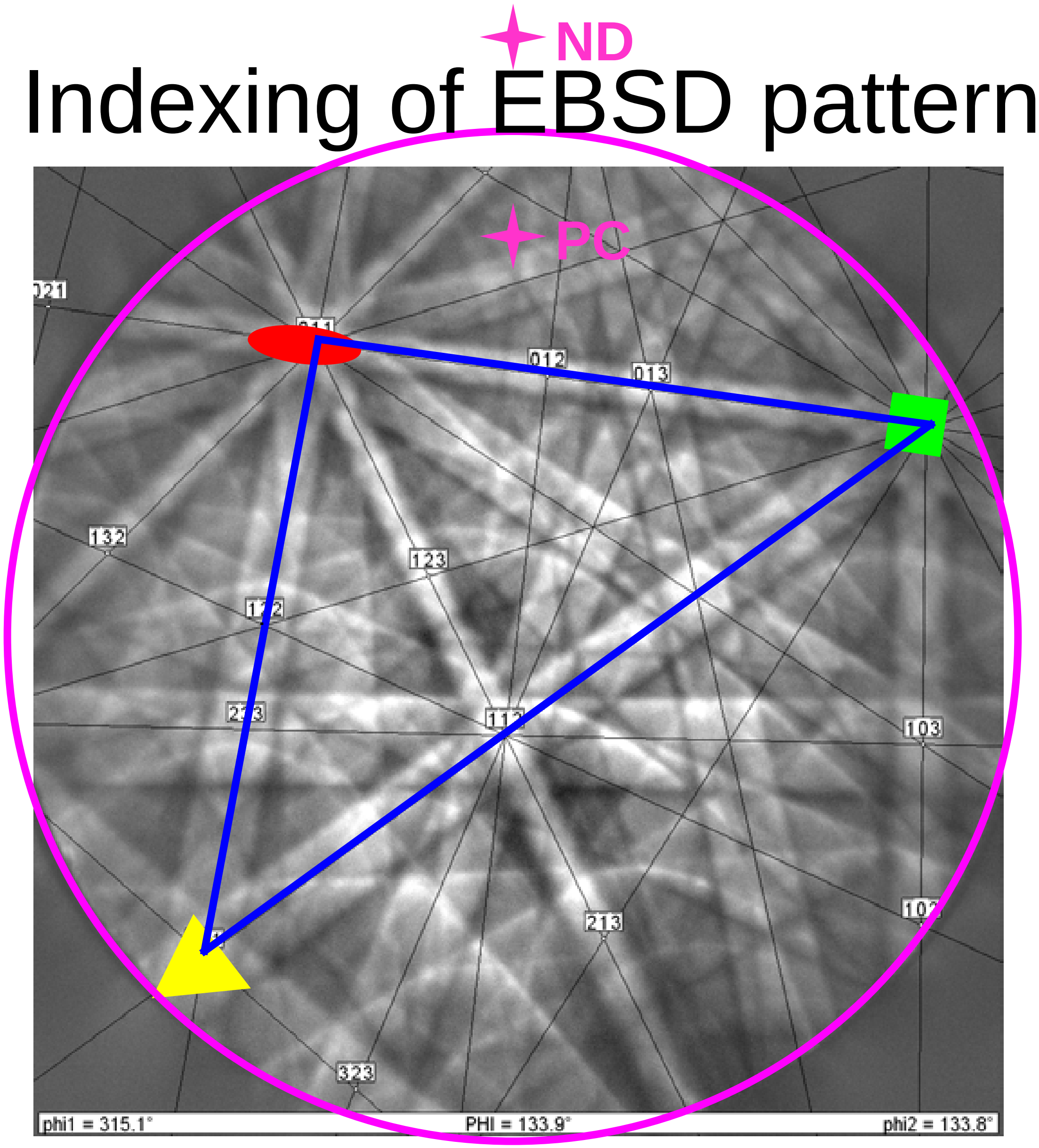

Nickel (fcc)

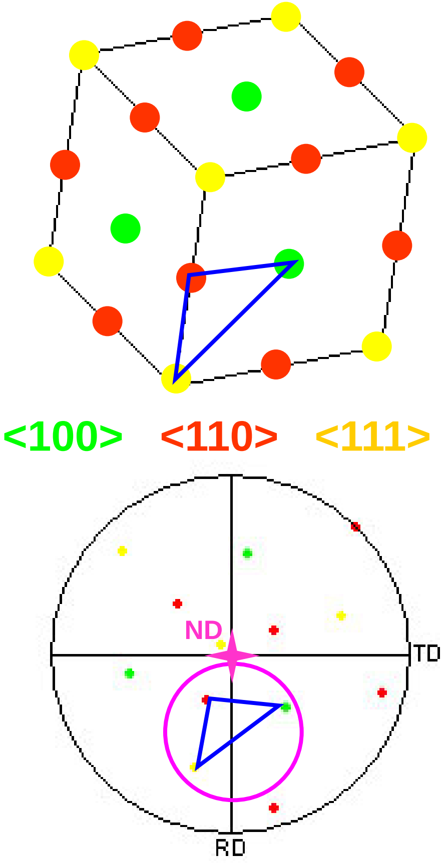

Orientation mapping

- Many orientation measurements with spatial correlation
  - Band detection
  - Pattern indexing & orientation (+ phase) determination
  - Raster scan of e-beam relative to sample

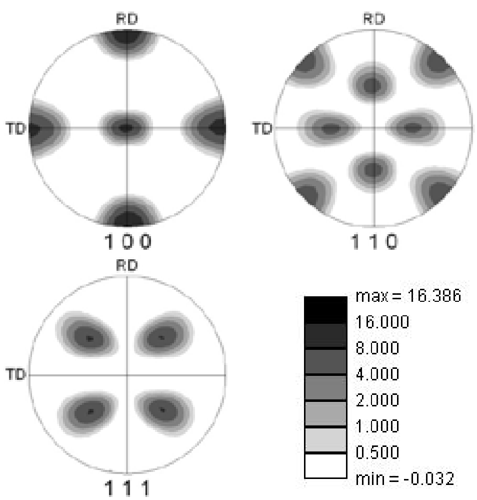

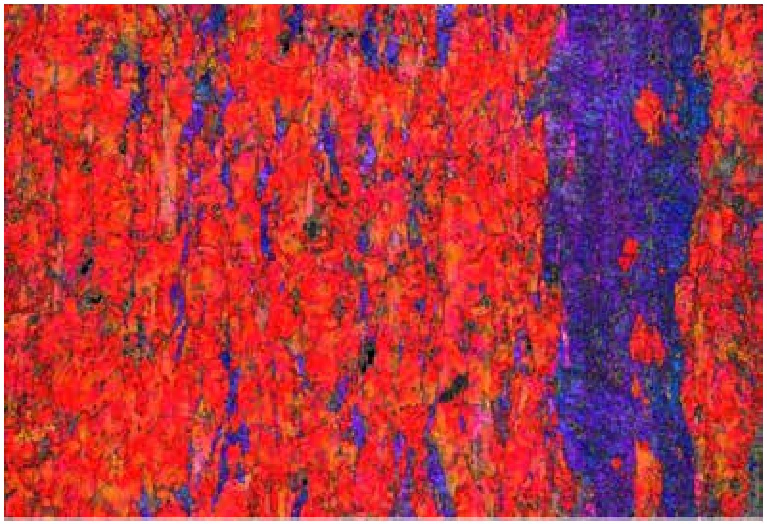

Cu foil O21b1c: 300 x 250 @ 0.5mm

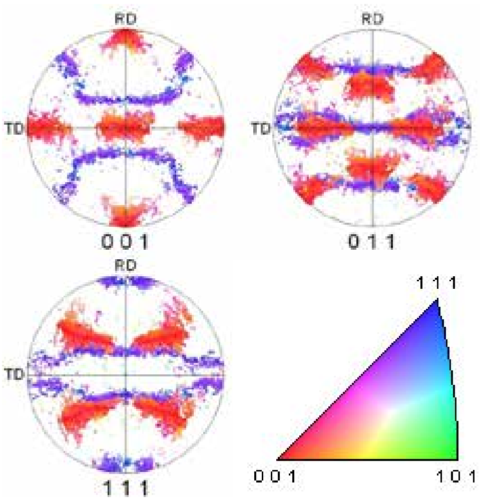

Simons et al. / Solid State Phenomena 105 (2005) 465-475

Macro - micro - nano

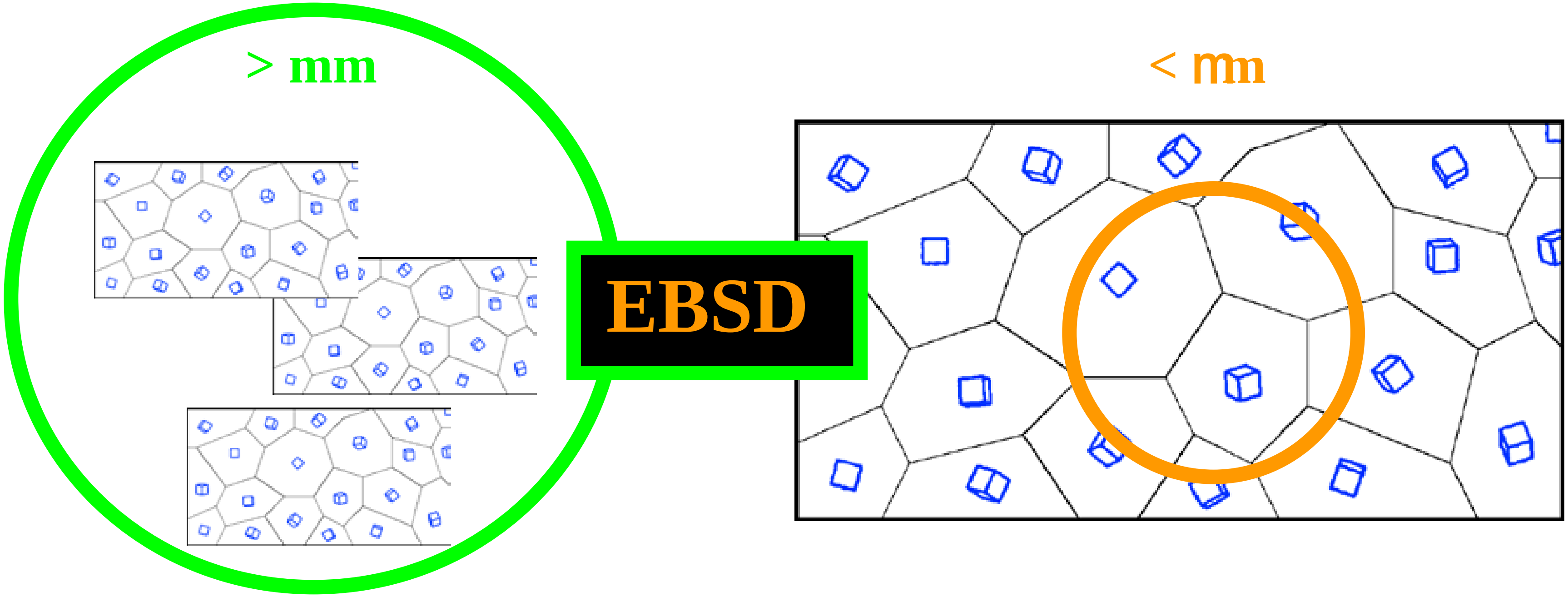

- statistical (bulk) information
- homogeneity
- texture goniometry

  (X-rays, neutrons)

- local (site-specific) information
- heterogeneity
- microscopy

  (light, electrons)

Grain size selective analysis – quartz mylonite

Color by orientation

Large grains

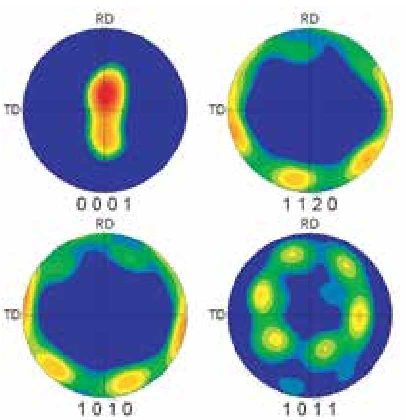

Color by grain size + grain boundaries

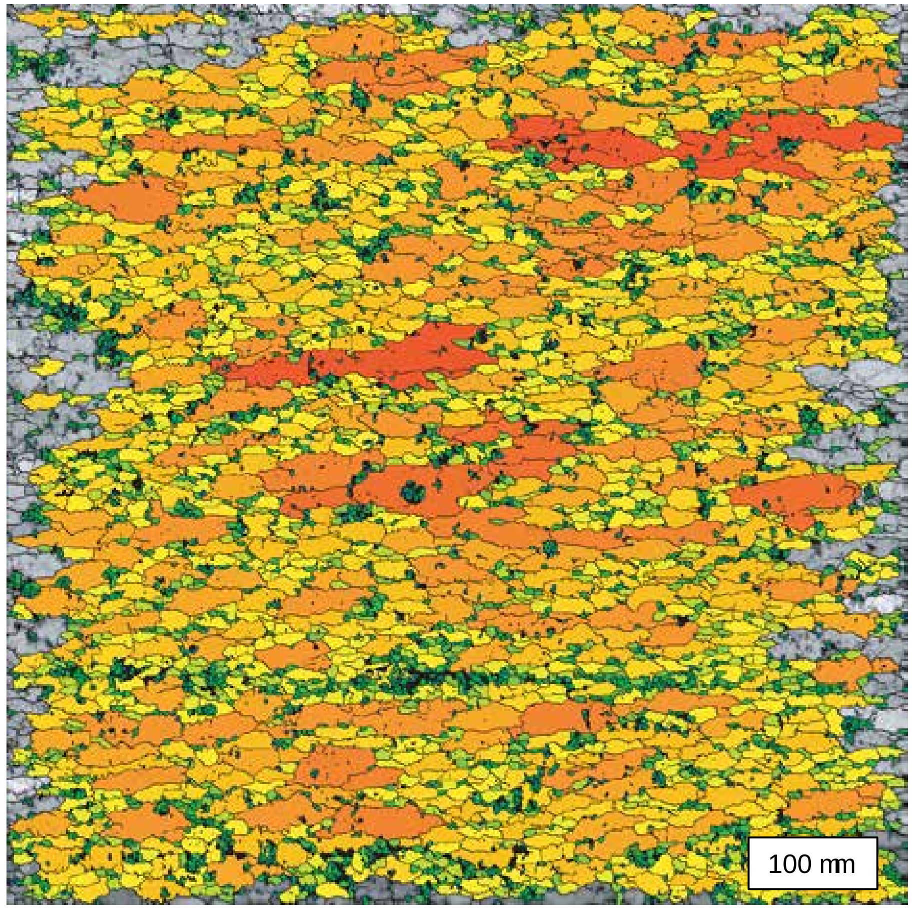

J FitzGerald, N Mancktelow, G Pennacchioni, K Kunze
GEOLOGY *34(2006) 369-372*

Color by orientation

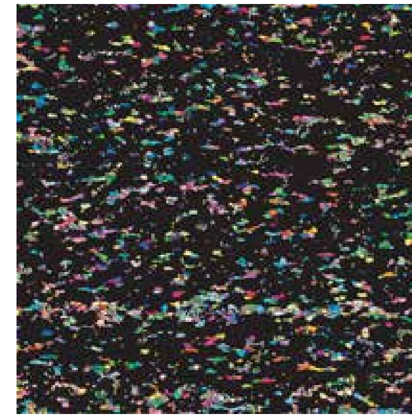

Small grains

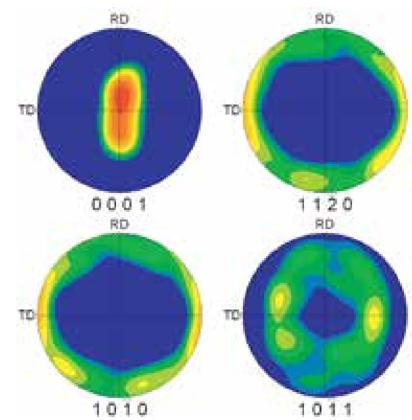

ETH zürich ScopeM

Analytical SEM

1. Introduction

2. X-ray spectroscopy
    a) Emission of X-rays
    b) Detection of X-rays (EDX)
    c) Detection of X-rays (WDX)

3. Electron back scatter diffraction (EBSD)
    a) general basics
    b) recent developments

EBSD detector technology
- speed and resolution

Phosphor scintillator + optics

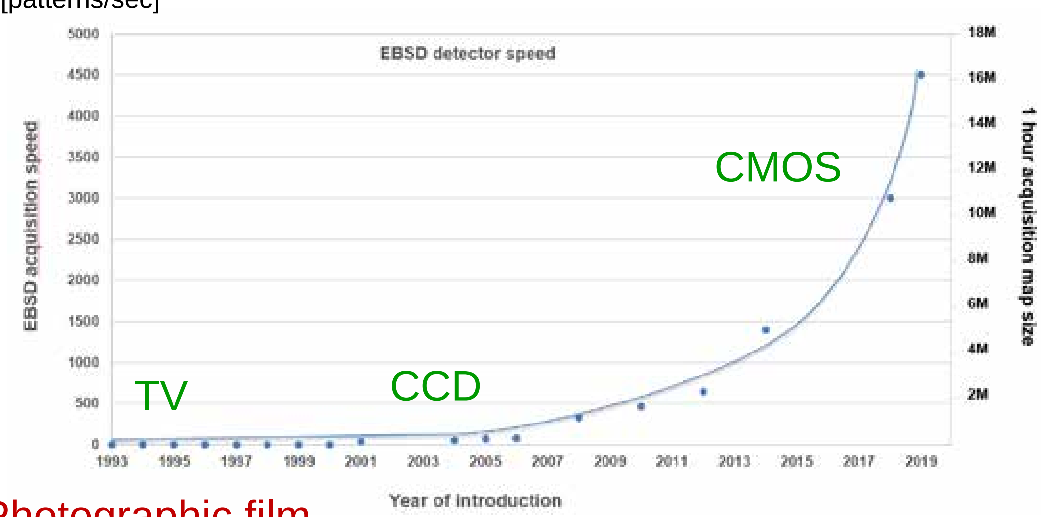

ß Photographic film

www.edax.com/products/ebsd/velocity-ebsd-camera
nano.oxinst.com/symmetry

Direct electron detector

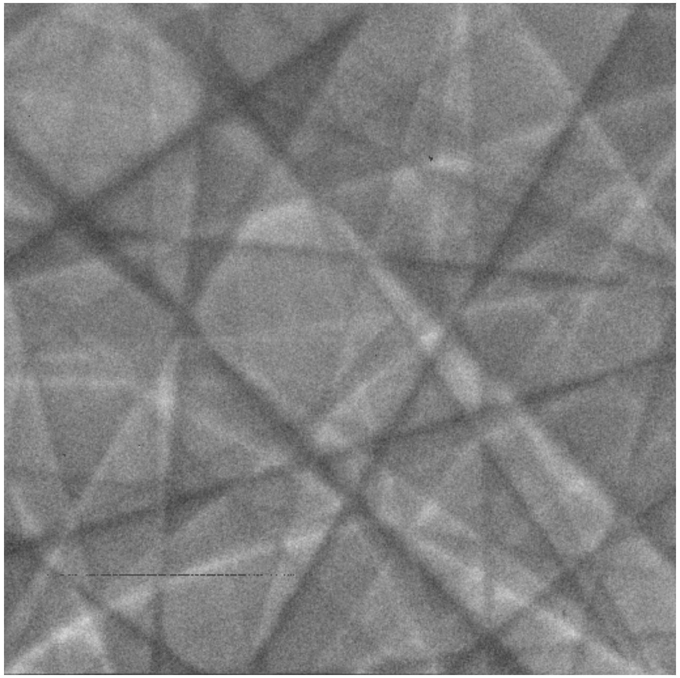

www.edax.com/products/ebsd/clarity-ebsd-detector-series

à *Higher sensitivity*
à *Lower kV and beam current*

Proper point group determination – breakdown of Friedel's law

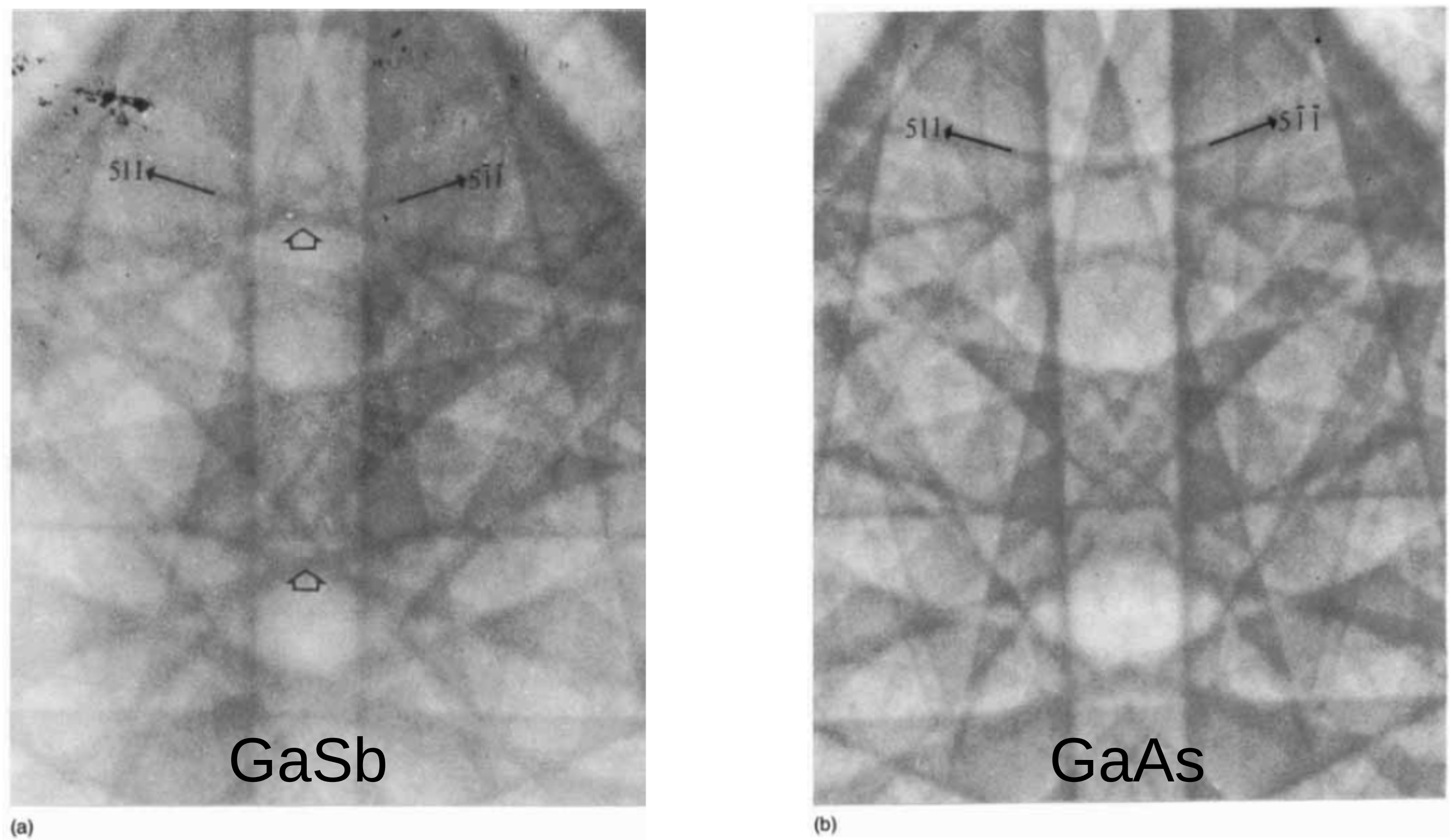

FIG. 7 BKP from GaSb illustrating distinct intensity differences between the reflections 511 and $5\bar{1}\bar{1}$, indicating that GaSb is noncentrosymmetric. (b) BKP from GaAs fails to show any intensity difference between the reflections 511 and $5\bar{1}\bar{1}$ (arrows).

K.Z. Baba-Kishi & D.J. Dingley (1989) Scanning 11(6) 305–312
K.Z. Baba-Kishi & D.J. Dingley (1989) J Appl Cryst 22 189-200

Polarity-sensitive orientation mapping

GaP: zinc blende structure, space group F43m

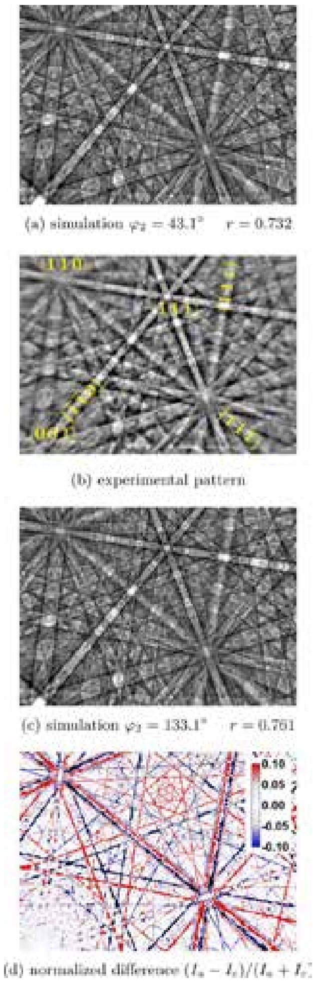

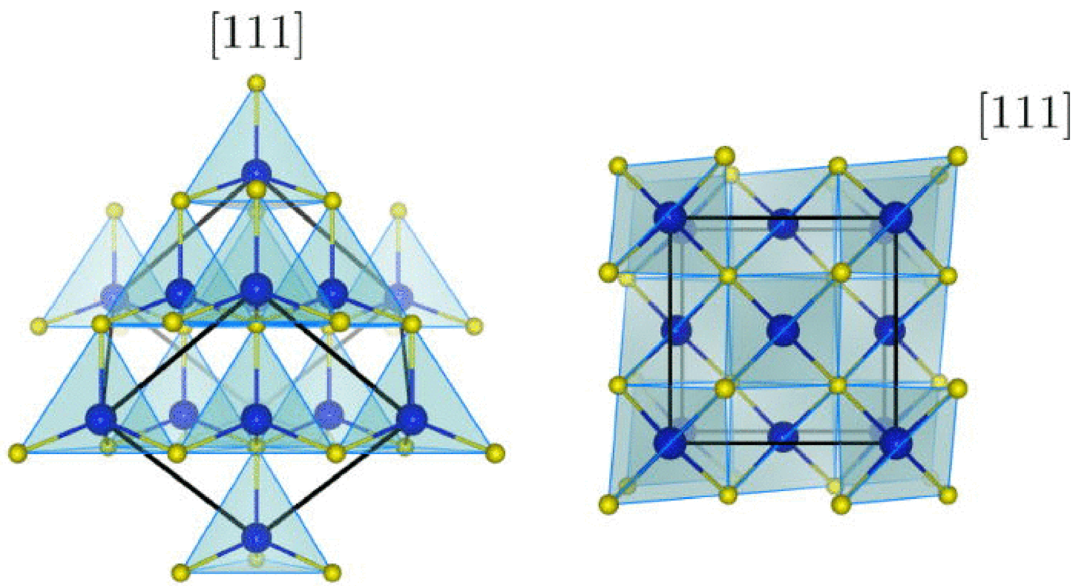

FIG. 1. Non-centrosymmetric zinc-blende-type structure of GaP (Ga: large, blue; P: small, yellow). Left: view along [$\bar{2}$11], with [111] up. Right: view along [001], with [010] up. The [111] marks the cube diagonal.

A. Winkelmann & G. Nolze (2015)
Appl. Phys. Lett. 106, doi:10.1063/1.4907938

Polarity-sensitive orientation mapping

GaP: zinc blende structure, space group F43m

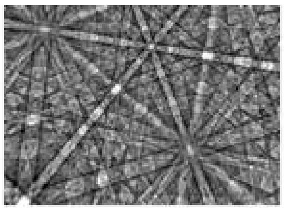

(a) simulation $\varphi_2 = 43.1°$ $r = 0.732$

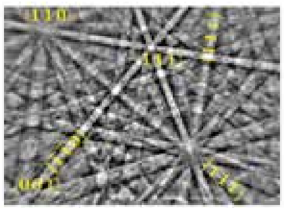

(b) experimental pattern

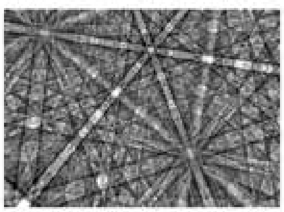

(c) simulation $\varphi_2 = 133.1°$ $r = 0.751$

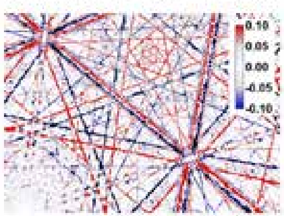

(d) normalized difference $(I_a - I_c)/(I_a + I_c)$

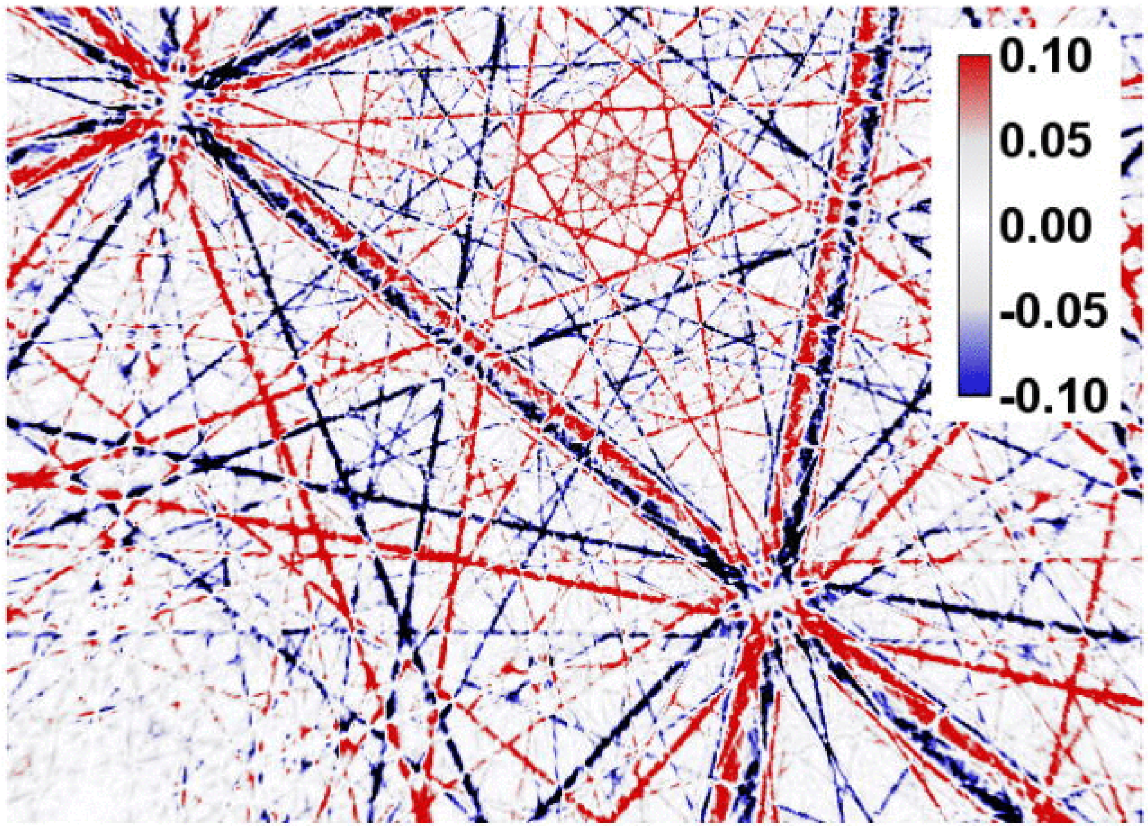

(d) normalized difference $(I_a - I_c)/(I_a + I_c)$

A. Winkelmann & G. Nolze (2015)
Appl. Phys. Lett. 106, doi:10.1063/1.4907938

Spherical (and dictionary) indexing

Master pattern of Kikuchi sphere

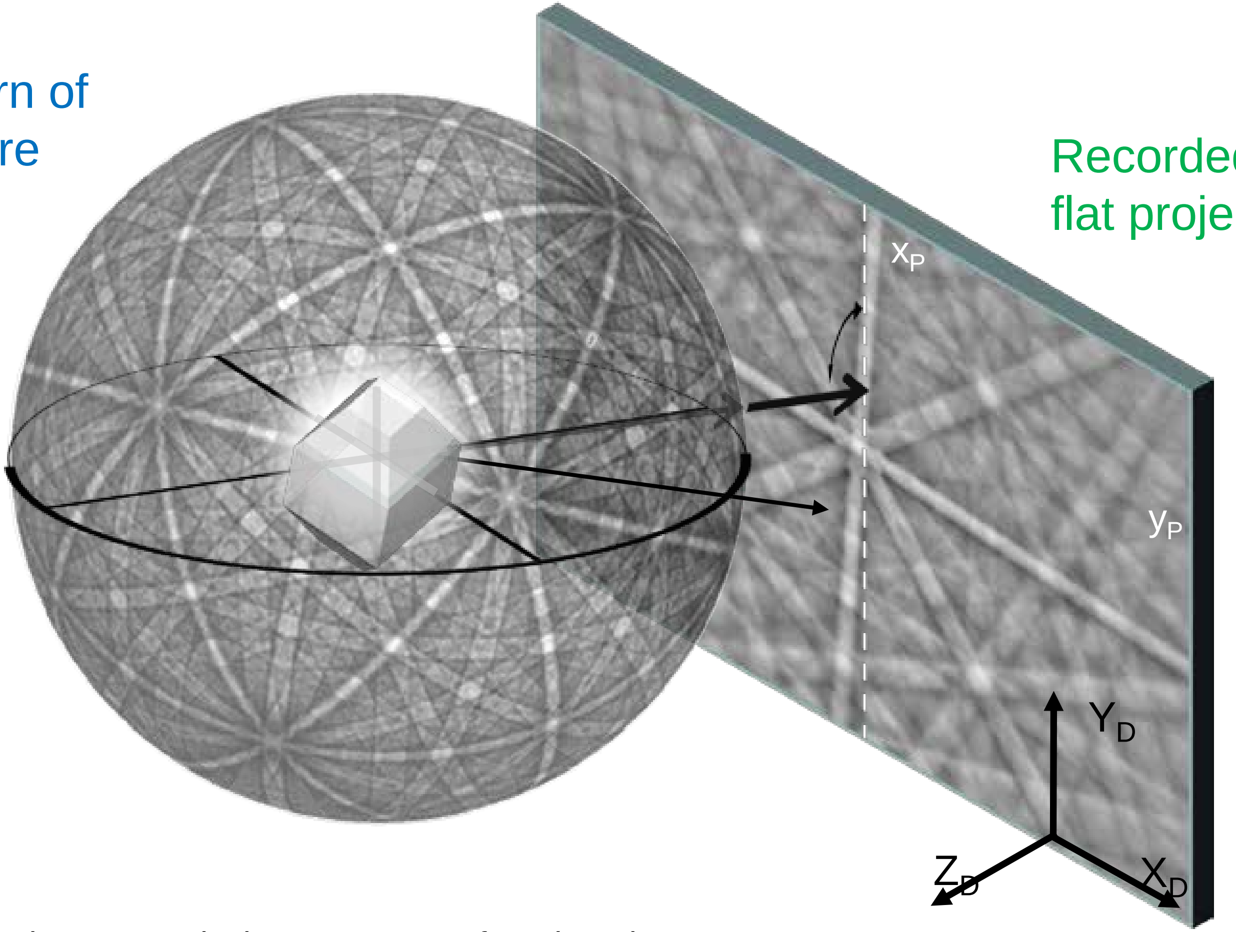

Recorded pattern on flat projection screen

Lenthe, W. C., Singh, S., & De Graef, M. (2019).
A spherical harmonic transform approach to the indexing of electron back-scattered diffraction patterns.
Ultramicroscopy, 207, 112841.

Spherical (and dictionary) indexing

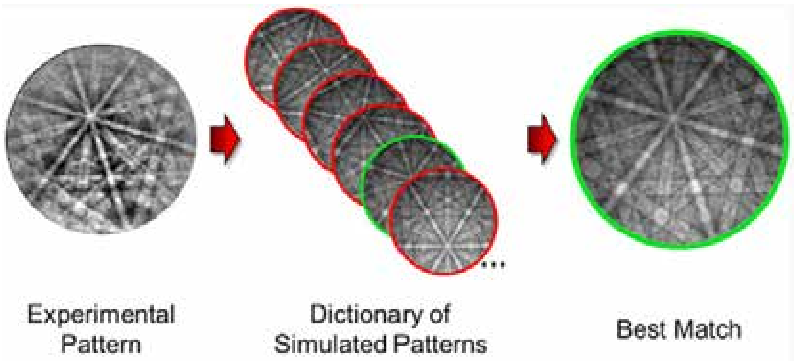

Figure 2. Schematic for dictionary indexing.

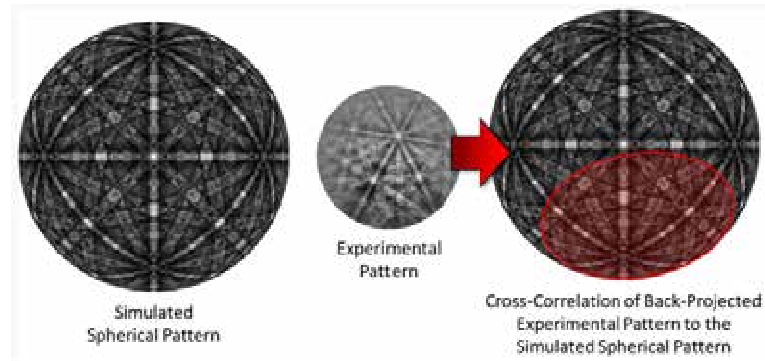

Figure 3. Schematic for spherical indexing.

- pre-calculation of master pattern(s) from atomic structure via simulations based on dynamic scattering

- Data collection and recording all experimental EBSD patterns

- Post-processing on stored data

à Demanding in resources of storage and GPU power

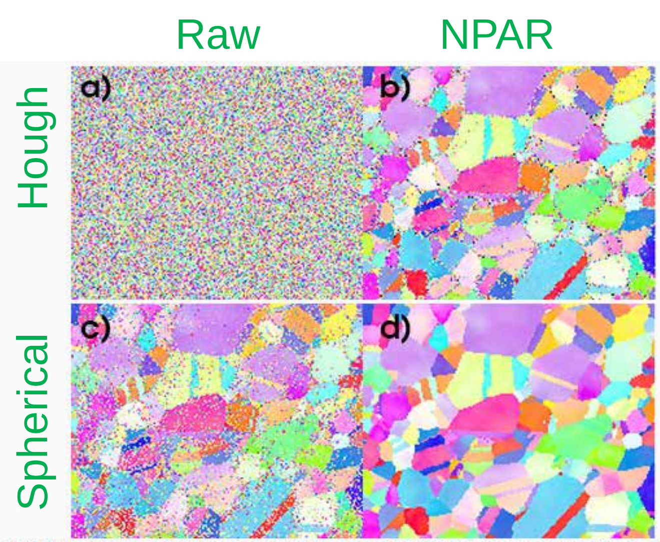

Figure 5. a) Raw pattern and b) NPAR pattern using Hough indexing and c) raw pattern and d) NPAR pattern using spherical indexing with a bandwidth of 127.

https://www.edax.com/resources/application-notes/spherical-indexing-in-oim-analysis

ETH zürich

ScopeM

TKD = Transmission Kikuchi Diffraction

Journal of Microscopy

Journal of Microscopy, Vol. 245, Pt 3 2012, pp. 245–251 doi: 10.1111/j.1365-2818.2011.03566.x
Received 11 July 2011; accepted 9 October 2011

Transmission EBSD from 10 nm domains in a scanning electron microscope

R.R. KELLER & R.H. GEISS
Materials Reliability Division, National Institute of Standards and Technology, Boulder, CO 80305, U.S.A.

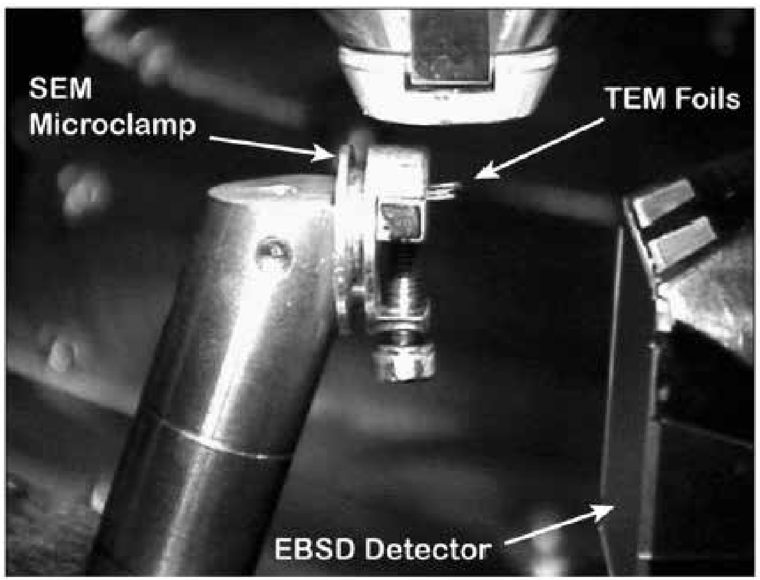

Fig. 1. In-chamber CCD TV camera image showing the experimental set up for SEM-TKD, with the pretilted EBSD sample holder, the TEM foils held in a micro-clamp in a horizontal position, and the EBSD detector to the right.

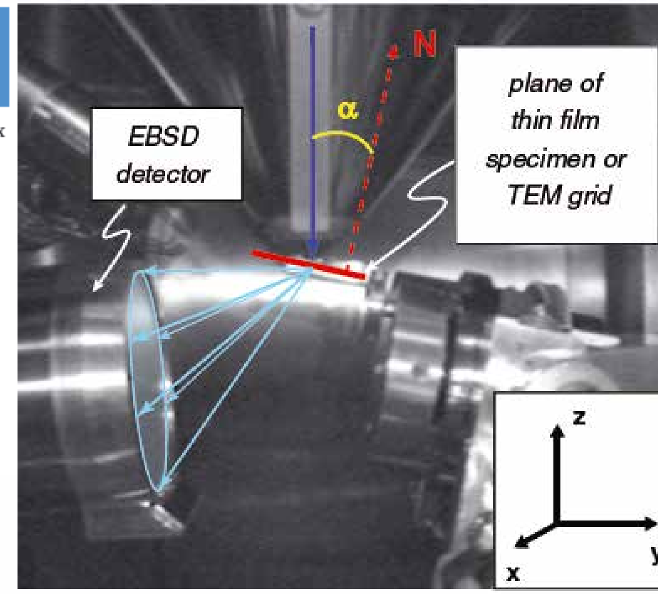

Fig. 1. Infrared image showing relative positions of incident electron beam (dark blue), thin specimen (red), transmitted electrons (light blue) and EBSD camera for collecting t-EBSD patterns in the SEM.

Ultramicroscopy 120 (2012) 16–24

Contents lists available at SciVerse ScienceDirect

Ultramicroscopy

journal homepage: www.elsevier.com/locate/ultramic

ELSEVIER

Orientation mapping of nanostructured materials using transmission Kikuchi diffraction in the scanning electron microscope

Patrick W. Trimby *
Australian Centre for Microscopy & Microanalysis, The University of Sydney, Madsen Building F09 Sydney, NSW 2006, Australia

n-Ti

nTi_3h_ad_cs_scan7
10 um x 10 um x 10 nm

1. FSE image
2. IQ
3. IPF-TD + IQ
4. IPF-ND + IQ
5. IPF-ND + GB

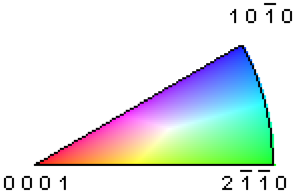

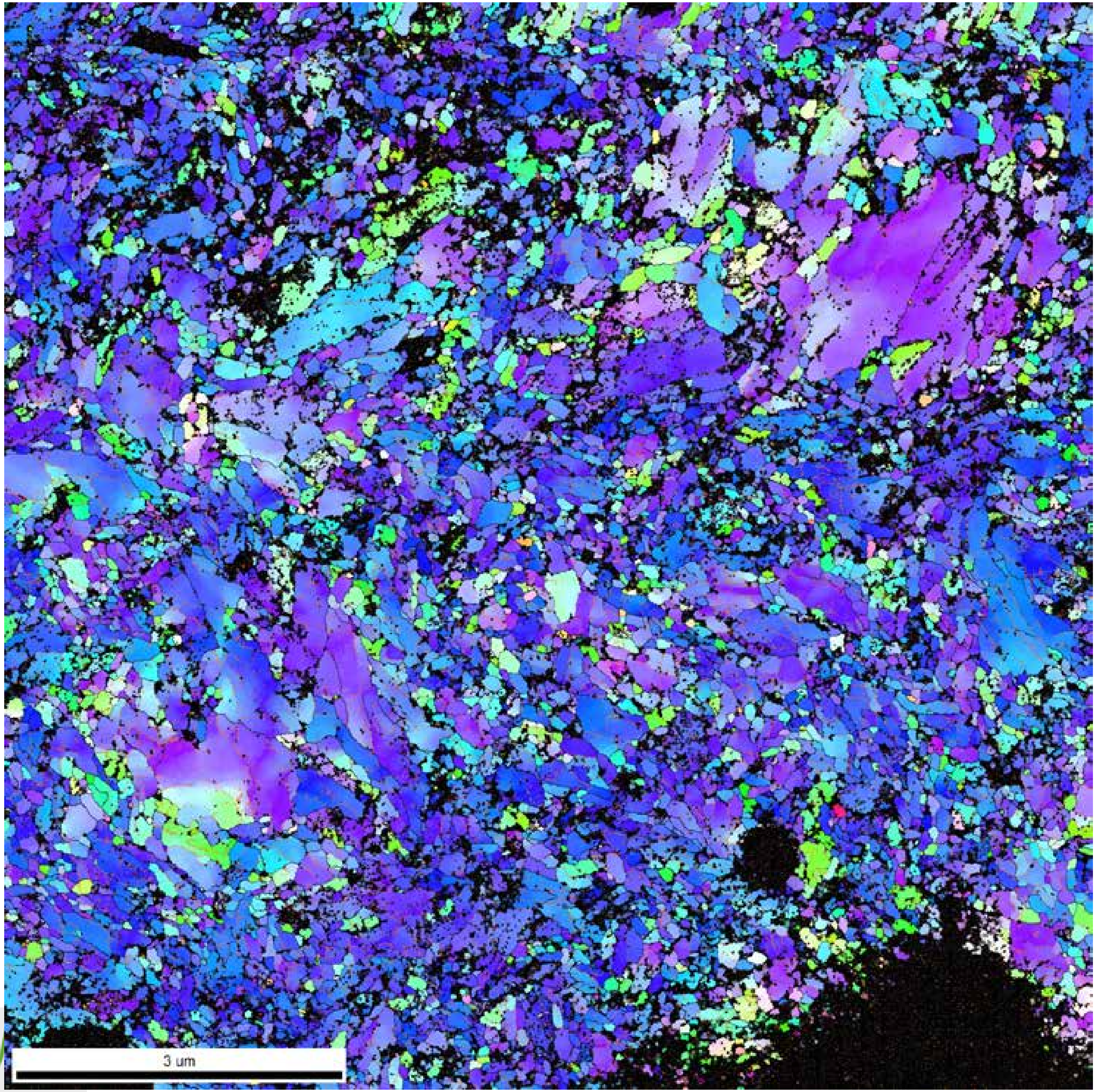

Tilt-free detection geometry

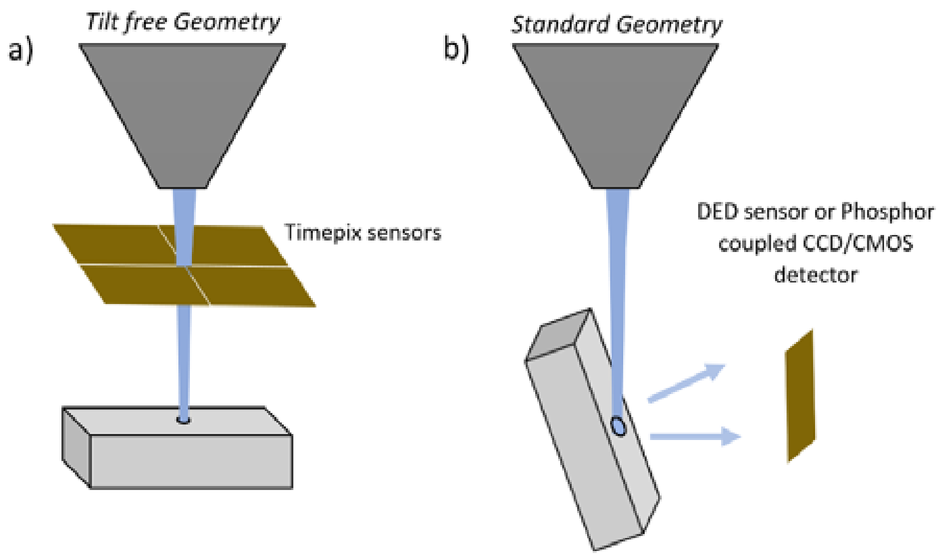

Fig. 2. A schematic diagram of a) the tilt-free detector geometry and b) a standard detector geometry for reference.

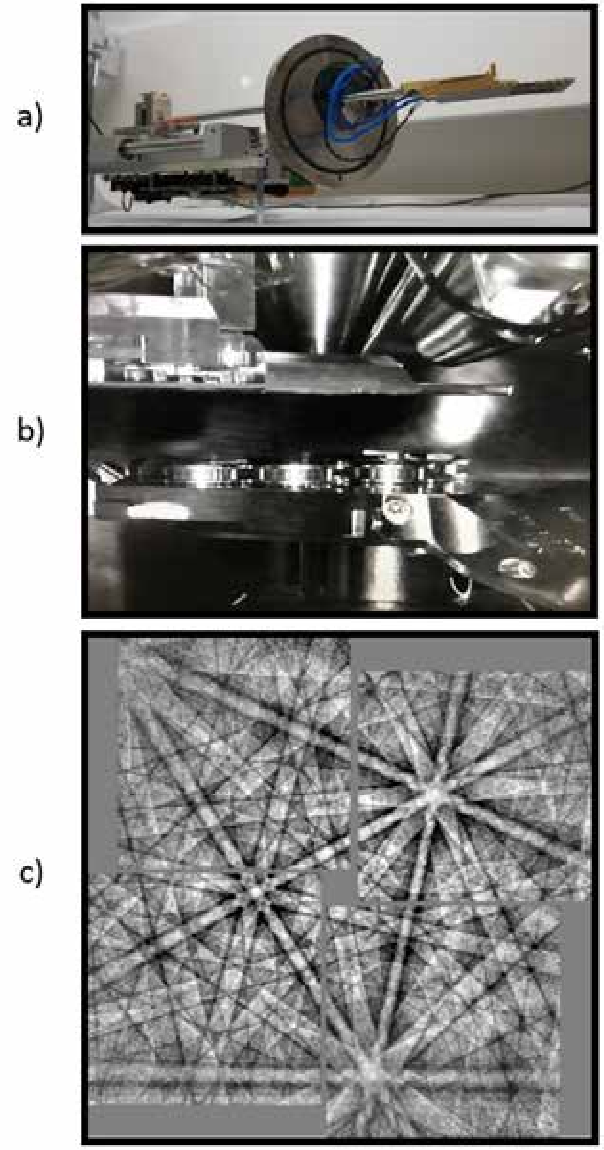

Fig. 3. An overview of the tilt-free direct detect EBSD detector with a) an image of the complete hardware design with electronics external to the SEM chamber, b) operational image of tilt-free geometry detector within the SEM chamber and c) an example Ni EBSP collected in the tilt-free geometry at 20 kV with a 2 second exposure time.

A.L. Marshall et al. Ultramicroscopy 226 (2021) 113294
doi: 10.1016/j.ultramic.2021.113294

ETH zürich ScopeM

EBSD – further topics – not covered

- Sample preparation requirements
- Multiple phases
- Pseudo-symmetry, lattice distortions
- Elastic strain: HR-EBSD
- Plastic strain: GND
- TEM-like dislocation contrast: ECCI
- Texture & anisotropic properties
- Grain & grain boundary characterization
- Data treatment and post-processing
- …

Summary: Analytical SEM

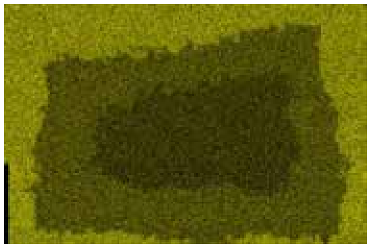

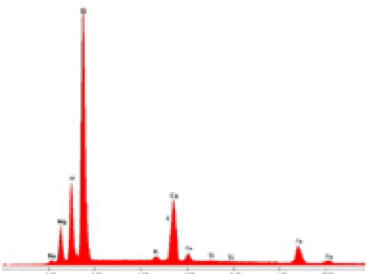

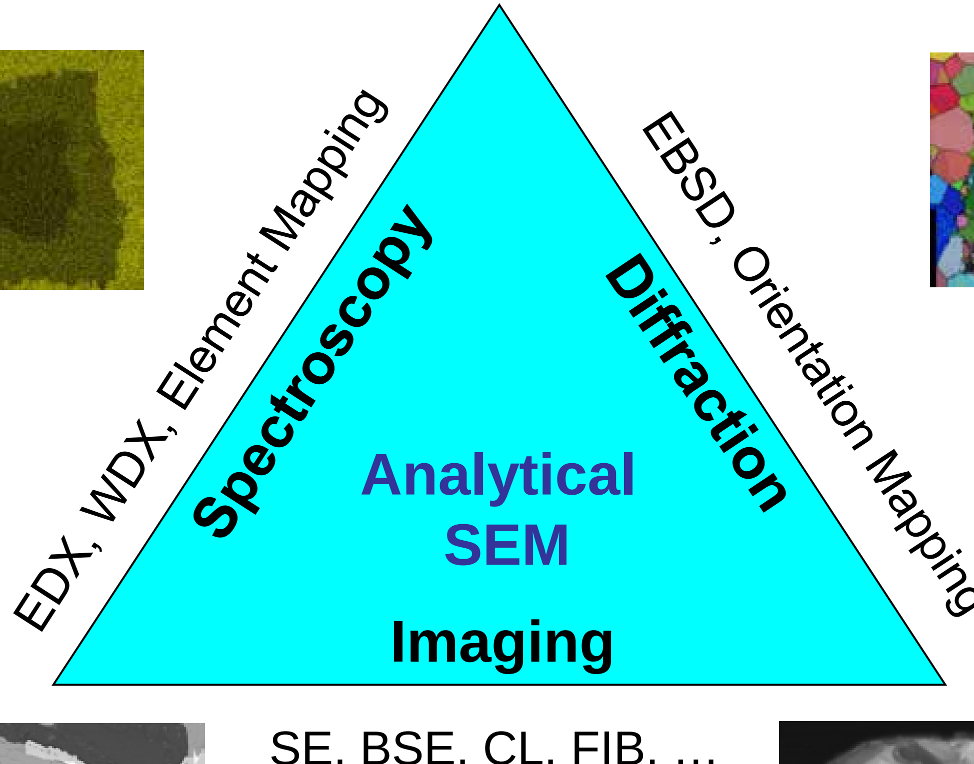

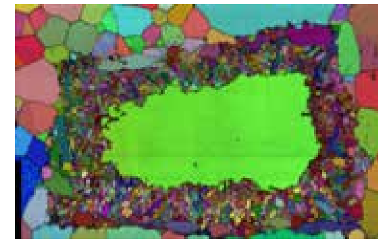

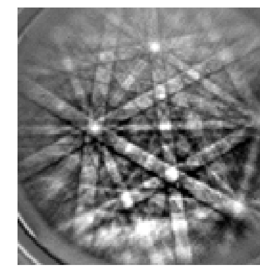

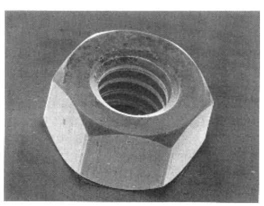

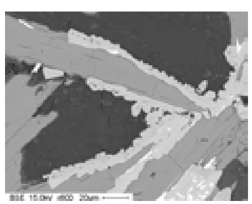

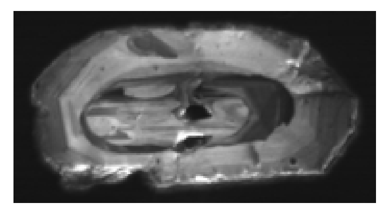

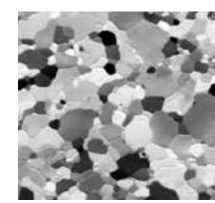

Analytical SEM – pushing resolution

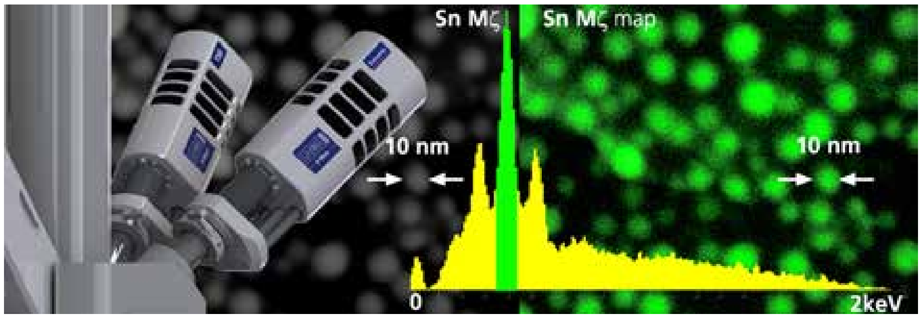

Low kV

- Reduced interaction volume
- Enhanced surface sensitivity on bulk samples
- FEG-SEM
- Windowless detectors, DED

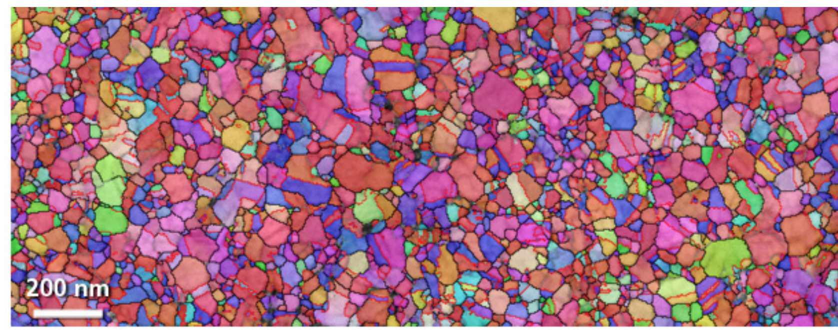

A cleaned inverse pole figure map showing detailed grain structure, even the smallest grains have been resolved. There is a prevalence of sigma 3 CSL boundaries (shown in red). Click the image to expand full scale in a new window.

Thin samples

- Reduced interaction volume
- STEM-EDX and -TKD available in SEM

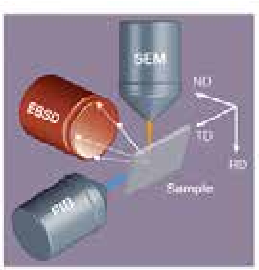

3D

- FIB-SEM
- Various signals: BSE, EDS, EBSD
- Fast acquisition

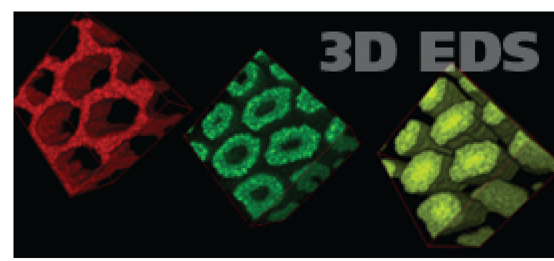

www.oxford-instruments.com